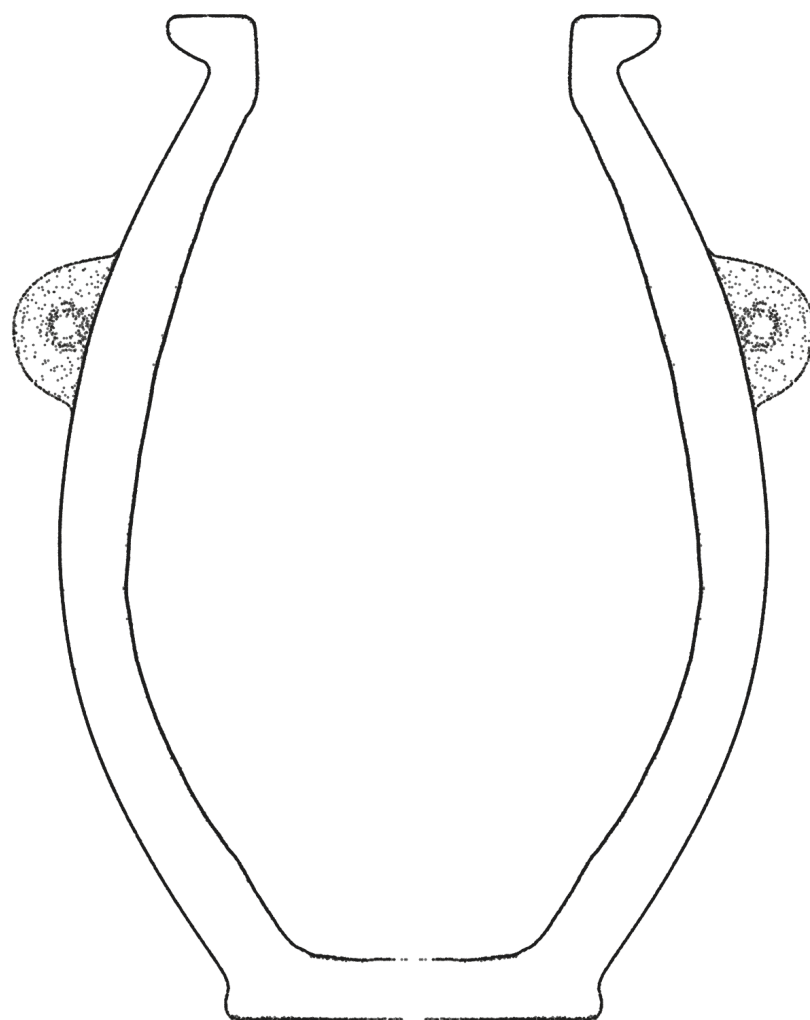
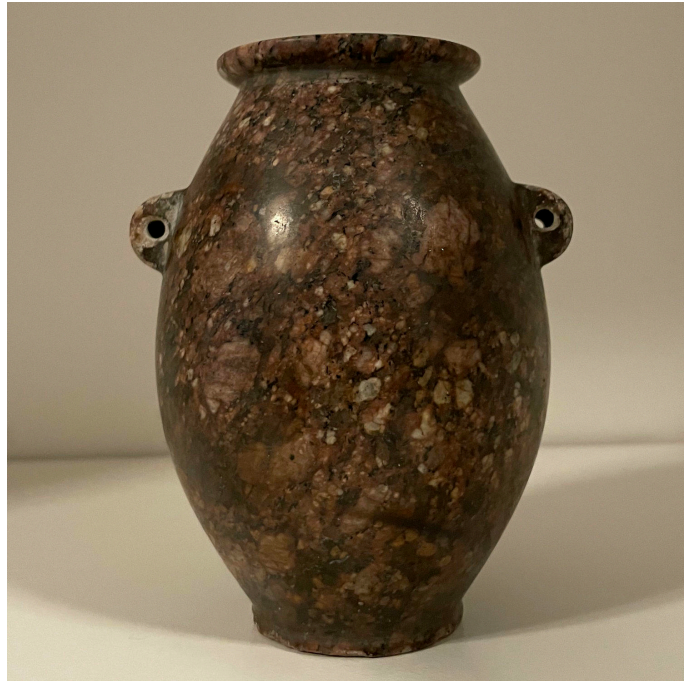


PV001 - Tall Ovoid Jar

An Exploration of Precision



Author: Stine Gerdes, arcsci.org
License: Creative Commons BY-NC-SA 4.0
Date: 2025-03-15
Version: 01.11



Artifact Foundation

Contents

Artifact Information	2
Alignment In The Cartesian Coordinate System	3
Precision	5
Circularity	5
Concentricity	25
Coaxiality	37
Surface Variability	40
Precision Score Of The Artifact	47
Analysis Roadmap	49
Appendix A - Comparison Of Circularity Measurements (Z-plane vs. surface-perpendicular)	50
Appendix B - Comparison Of Concentricity Measurements (Z-plane vs. surface-perpendicular)	57

Artifact Information

Artifact Data

Collection	In private collection of Adam Young
Provenance ¹	Previously in collection of Mr. David Lewis, London UK, acquired in 1980s
Provenience ²	Unknown
Attribution	Egypt, 2nd-3rd Dynaty, c. 2900-2600 B.C.

Art dealer information

Ref.	28.34608
Description	Egyptian Early Dynastic Granite Amphora Jar, 2nd-3rd Dynasty, c. 2900-2600 B.C.
URL	

Maijers vessel classification³

Short classification	Tall Ovoid Jar
Long classification	The vessel is created in a closed form classified as a tall jar with a ovoid shape, it has a footed base and a raised blunt rim.

Physical properties

Precision score ⁴	1905
Height (approximate)	120 mm 4.72 in
Width (approximate)	96 mm 3.78 in
Material	Red Granite
Mohs Hardness ⁵	6 - 8 (Granite)
Weight	Unknown

Scan information

Source	Scanned by Artifact Foundation
Source file name	vase 2.stl
Scan method	CT
Scanner	CT - Zeiss Metrotom 1500
Rated scan accuracy	Not specified
Scan date	April 2023
Scanned by	Zeiss
Mesh decimation	Topology-Preserving Quadratic Edge Collapse Decimation ⁶
Number of vertices	2 446 005
Mesh density ⁷	106 µm 4.16 thou
Max vertex distance	270 µm 10.620 thou
Min vertex distance	1 µm 0.056 thou
Vertices per cm ²	3301 (approximated)
Vertices per in ²	21 296 (approximated)

¹The verifiable chain of custody of an artifact

²The location or site where an artifact was recovered

³Vessel artifact classification developed by W. Arnold Maijer and described in his publication Masters of Stone, ISBN 978-90-829212-0-5

⁴The precision score metric is described in Precision Score Of The Artifact, p. 48

⁵The Mohs scale is an ordinal scale, from 1 to 10, describing the materials resistance to abrasion (the ability of harder material to scratch softer material)

⁶<https://arxiv.org/pdf/2411.16874.pdf>, <https://www.cs.cmu.edu/~garland/Papers/quadrics.pdf>

⁷Median distance between vertices

Alignment In The Cartesian Coordinate System

For precise and valid measurements of the vessel's geometry to be possible, the points of the scanned dataset must first and foremost be placed optimally in a Cartesian coordinate system. Several alignment methods and algorithms have been tested on a number of different vessels to determine the best way to achieve optimal alignment.

Any misalignment of the artifact will increase the error of the precision measurements, due to the distortion/wobble effect caused by the misaligned object. To visualize this distortion, we can consider a representation of the three-dimensional point cloud data, folded to a two-dimensional plane. This folded representation is obtained by rotating all scanned points around an assumed center axis to $y = 0$, $x > 0$, thus resulting in a two-dimensional profile representation of all scanned vertices in the object.

Figure 1 illustrates this effect on a ideal ellipsoid. In the first image, the ellipsoid is perfectly aligned, resulting in a narrow and precise two-dimensional folded profile. As misalignments are introduced, the two-dimensional profile increases in width, visually showing the distortion, causing the error in the precision measurements to increase. While easy to understand visually, this distortion can also be objectively quantified, and as such used to compare the fitness of different assumed center axes against each other, and further to create an automated and solid process for optimal Cartesian alignment of the scan data.

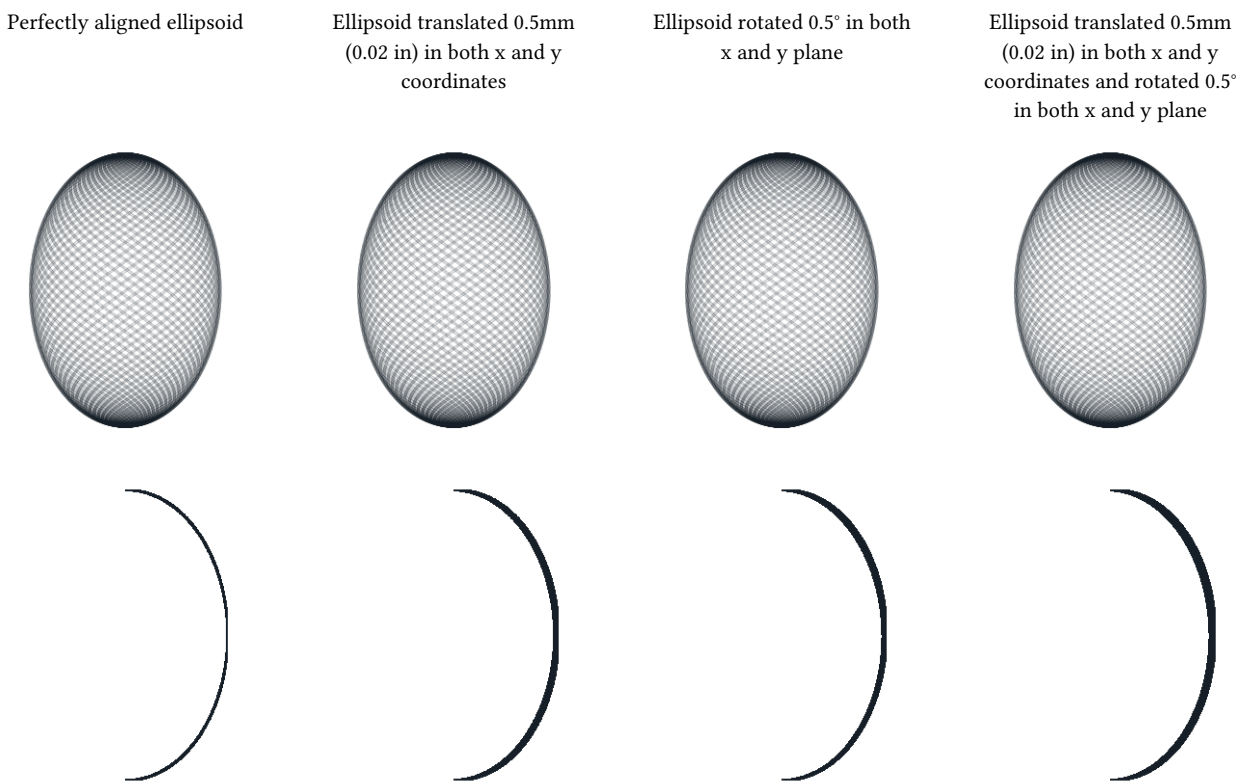


Figure 1: Distortion caused by a misalignment of the artifact

In contemporary metrology analysis of modern production objects, it is common to align the object in a Cartesian coordinate system by fitting a flat surface of the object to a reference plane in the coordinate system, cylindrical features to an ideal cylinder etc., or by using specific markers placed on the object in the design process. This methodology, however, is inadequate for the ancient objects in question. Most scanned artifacts, do not have a valid flat surface which could be aligned to a plane in the Cartesian coordinate system; most surfaces seem to be curved. Some artifacts do have a flat base, however this is often a worn area of the artifact and practical tests have shown that alignment to such surfaces will not produce optimal alignment of the scan data.

As conventional methods of alignment do not always yield good results with these types of artifacts, a more adequate method of alignment has been developed to enable precise measurements and statistical analysis of the scan data.

To find the optimal position of the vessel in the coordinate system, a range of rotation and translation tests are carried out to find the best fit of the central axis.

Based on the assumption that the analyzed object was created using a rotational process, and thus have symmetry around a central axis, the alignment of the artifact is carried out in a two-step process. An overview of this process is given below.

The artifact is placed in a Cartesian coordinate system, in an initially unaligned state. The first step in the alignment process estimates the central rotational axis of the vessel, by analyzing the coaxiality of thin cross-section slices of the vessel. The slices will be as thin as possible based on the mesh density of the scan, while still ensuring enough data points in each slice to be statistically valid.

For each slice, circular regression⁸ (estimate of best fit circle) is used to estimate the center point of this slice. Combined over the total Z-axis range of the vessel, these center points provide us with an indicator of the incline and position of the vessel's central axis.

The next step will optimize the center axis alignment by progressively minimizing the deviation (perpendicular to the surface curvature) of the two-dimensional profile, see Figure 1. By ascertaining and comparing the resulting fit of many thousands of different potential rotations, the best fit alignment of the scan data can be estimated, and an optimal center axis (in relation to the data points) can be reconstructed. The actual three-dimensional point-cloud is then aligned to this axis, by rotating and translating the scanned data points to match the Z-axis of the Cartesian coordinate system.

⁸Circle regression algorithm used: Kenichi Kanatani, Prasanna Rangarajan, "Hyper least squares fitting of circles and ellipses" Computational Statistics & Data Analysis, Vol. 55, pages 2197-2208, (2011)

Precision

To explore the manufacturing precision of the artifact in depth, the following analysis have been carried out:

- Circularity around the axis of symmetry is examined in detail at selected cross-sections.
- Overall circularity around the axis of symmetry is measured for the full height of the vessel (areas of the vessel with extensive damage are not taken into account for this metric).
- Concentricity of the vessel between selected cross-sections are examined in detail to determine if the existence of an axis of rotation in the manufacture of the object can be established.
- The coaxiality of the vessel is analyzed to explore the precision of the central axis of the object.
- The surface variability is analyzed and visualized on through a heatmap.

Circularity

Circularity is the measurement of how round the surface of an object is, optionally in reference to a datum axis. The *circularity tolerance* is the radial distance of two circles, each with their centers in the datum axis, and each of them conforming, respectively, to the minimum and maximum deviations of the data-set to a true circle, see Figure 2.

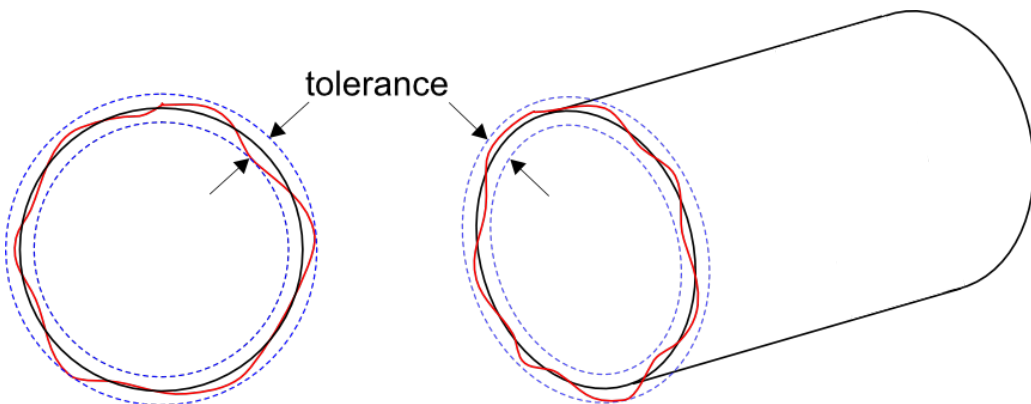


Figure 2: Circularity tolerance.

Circularity is examined at different cross-sections of the vessel, using the established Z-axis as the datum axis (axis of symmetry). The distance between the scanned points in the local datum plane is measured to determine the range between the two concentric circles encompassing the measured points, see Figure 3.

Referencing all of the individual circularity measurements to the global (reconstructed) axis of symmetry of the object, allows us to ascertain not only circularity of local features of the object, but how well circularity was *maintained* over the entire manufacturing process. This is an important distinction, which may be able to provide valuable insights into requirements of the construction methods. For reference, and seeing that the variance in local circularity also holds interest, measurements of circularity of the vessel without reference to the axis of symmetry can additionally be found in the Concentricity, p. 26.

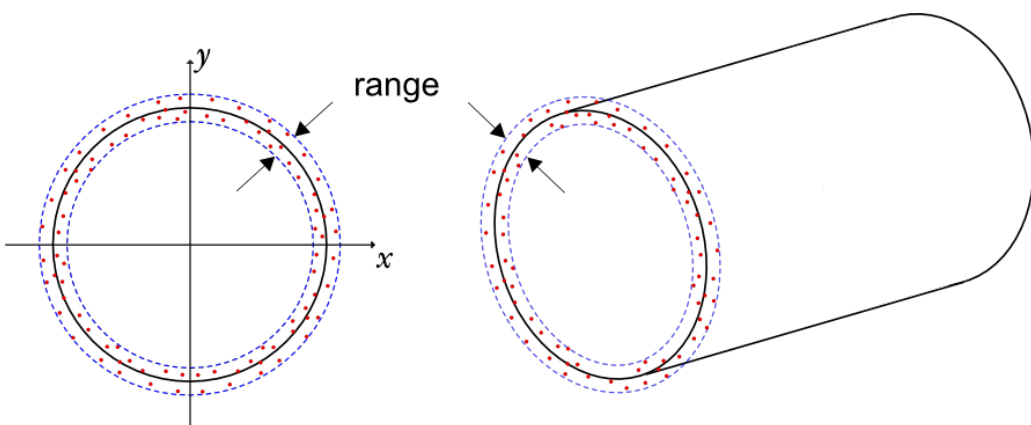


Figure 3: Circularity measurements.

If the circularity is determined from slices of the vessel exclusively in the *Z-plane* (actually measuring the cylindricity of a very thin slices of the vessel, in an attempt to approximate circularity), this would - in some areas - introduce significant distortion (increasing measurement errors) in the samples, due to the curvature of the vessel's surface.

Each sample slice of the vessel is therefore obtained perpendicular to the surface curvature, see Figure 5 to Figure 14. The measurements are taken conservatively without filtration of potential outliers.

To explore the potential distortion caused by obtaining samples in the Z-plane only, please refer to Appendix A, where measurements in the Z-plane and measurements perpendicular to surface curvature are compared side by side.

Detailed circularity measurements of selected points

Circularity measurements across a range of selected slices of the vessel (see Table 1) have been analyzed in-depth, and detailed plots of each measurement is provided. Furthermore, full circularity measurements are shown for each available scanned surface including a detailed plot to visualize the circularity of all areas of the vessel.

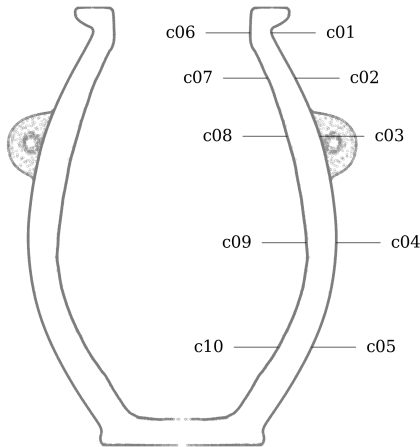


Figure 4: Circularity measurement sample location on PV001.

Metric

Tag	Area	Measured deviation ⁹	Residuals				Sample size	Slice		
			Range	RMSD ¹⁰	MAD ¹¹	SD		Height	Z coord.	Radius ¹²
		mm	mm	mm	mm	mm	mm	mm	mm	mm
c01	exterior	$\varnothing 49.103 \pm 0.069$	0.114	0.019	0.012	0.019	473	0.100	113.516	24.551
c02	exterior	$\varnothing 62.221 \pm 0.075$	0.128	0.025	0.019	0.025	585	0.100	101.108	31.110
c03	exterior	$\varnothing 75.848 \pm 0.101$	0.197	0.036	0.024	0.035	612	0.100	85.163	37.924
c04	exterior	$\varnothing 84.772 \pm 0.081$	0.141	0.019	0.013	0.017	921	0.100	55.890	42.386
c05	exterior	$\varnothing 71.251 \pm 0.065$	0.114	0.017	0.012	0.017	711	0.100	27.256	35.626
c06	interior	$\varnothing 37.457 \pm 0.120$	0.194	0.037	0.029	0.037	531	0.100	113.516	18.728
c07	interior	$\varnothing 47.060 \pm 0.163$	0.255	0.033	0.021	0.033	676	0.100	101.108	23.530
c08	interior	$\varnothing 57.791 \pm 0.222$	0.319	0.036	0.023	0.035	1119	0.100	85.163	28.896
c09	interior	$\varnothing 68.374 \pm 0.142$	0.238	0.031	0.021	0.031	1305	0.100	55.890	34.187
c10	interior	$\varnothing 52.949 \pm 0.118$	0.230	0.033	0.023	0.033	878	0.100	27.256	26.475

Imperial

Tag	Area	Measured deviation ⁹	Residuals				Sample size	Slice		
			Range	RMSD ¹⁰	MAD ¹¹	SD		Height	Z coord.	Radius ¹²
		in	in	in	in	in	in	in	in	in
c01	exterior	$\varnothing 1.9332 \pm 0.0027$	0.0045	0.0007	0.0005	0.0007	473	0.0039	4.4691	0.9666
c02	exterior	$\varnothing 2.4496 \pm 0.0029$	0.0050	0.0010	0.0007	0.0010	585	0.0039	3.9806	1.2248
c03	exterior	$\varnothing 2.9861 \pm 0.0040$	0.0078	0.0014	0.0010	0.0014	612	0.0039	3.3529	1.4931
c04	exterior	$\varnothing 3.3375 \pm 0.0032$	0.0056	0.0007	0.0005	0.0007	921	0.0039	2.2004	1.6687
c05	exterior	$\varnothing 2.8052 \pm 0.0026$	0.0045	0.0007	0.0005	0.0007	711	0.0039	1.0731	1.4026
c06	interior	$\varnothing 1.4747 \pm 0.0047$	0.0076	0.0015	0.0011	0.0014	531	0.0039	4.4691	0.7373
c07	interior	$\varnothing 1.8528 \pm 0.0064$	0.0100	0.0013	0.0008	0.0013	676	0.0039	3.9806	0.9264
c08	interior	$\varnothing 2.2753 \pm 0.0087$	0.0126	0.0014	0.0009	0.0014	1119	0.0039	3.3529	1.1376
c09	interior	$\varnothing 2.6919 \pm 0.0056$	0.0094	0.0012	0.0008	0.0012	1305	0.0039	2.2004	1.3459
c10	interior	$\varnothing 2.0846 \pm 0.0046$	0.0090	0.0013	0.0009	0.0013	878	0.0039	1.0731	1.0423

Table 1: Detailed circularity measurements at selected samples of PV001.

Figure 5 to Figure 14 shows a detailed plots of each circularity measurement.

⁹Sample diameter $\varnothing \pm$ maximum measured deviation from measured radius

¹⁰Root mean square deviation (RMSD) also called Root mean square error (RMSE)

¹¹Median absolute deviation

¹²Median sample radius from z-axis

Graphical overview of circularity measurement c01

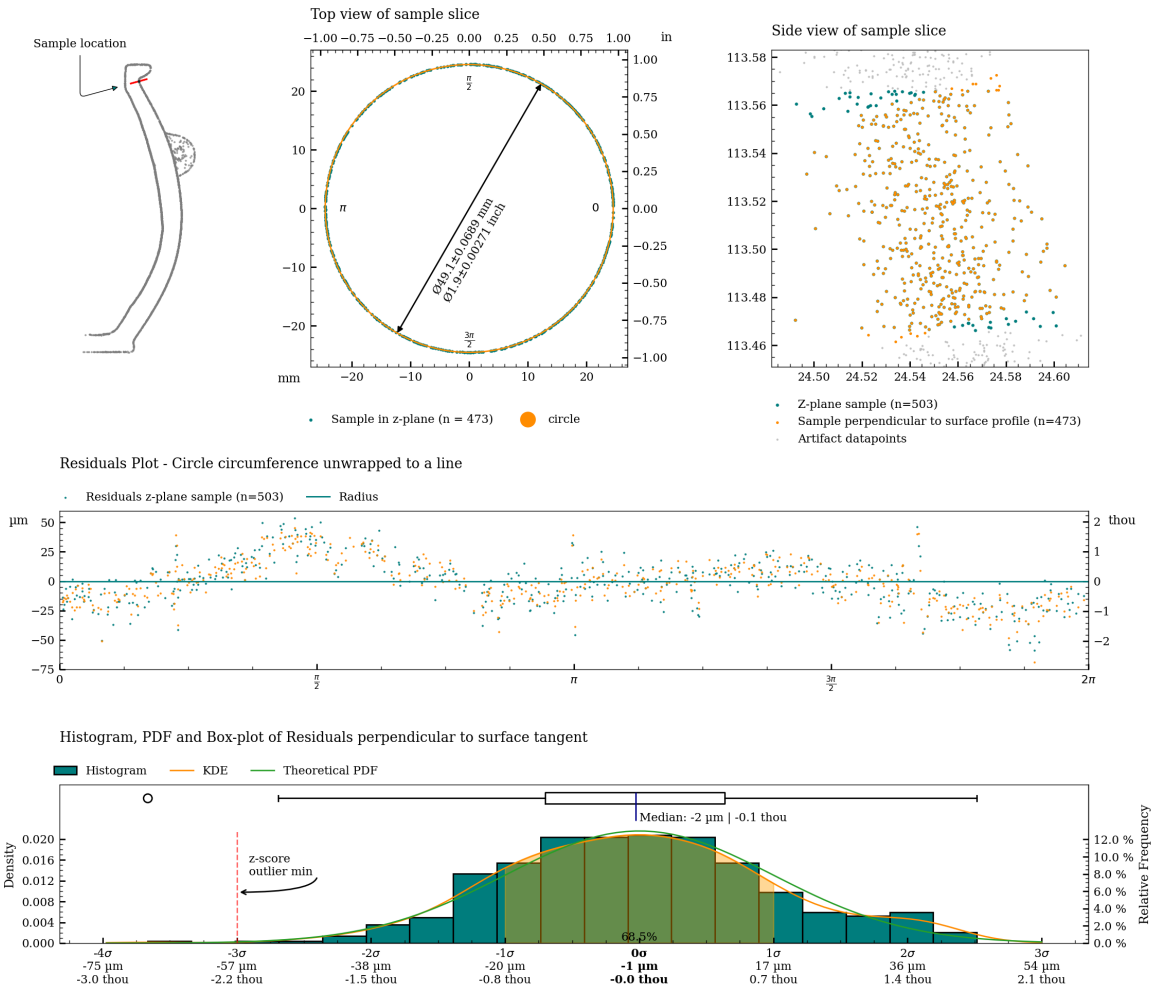


Figure 5: Charts with statistics for the measurement of c01.

Graphical overview of circularity measurement c02

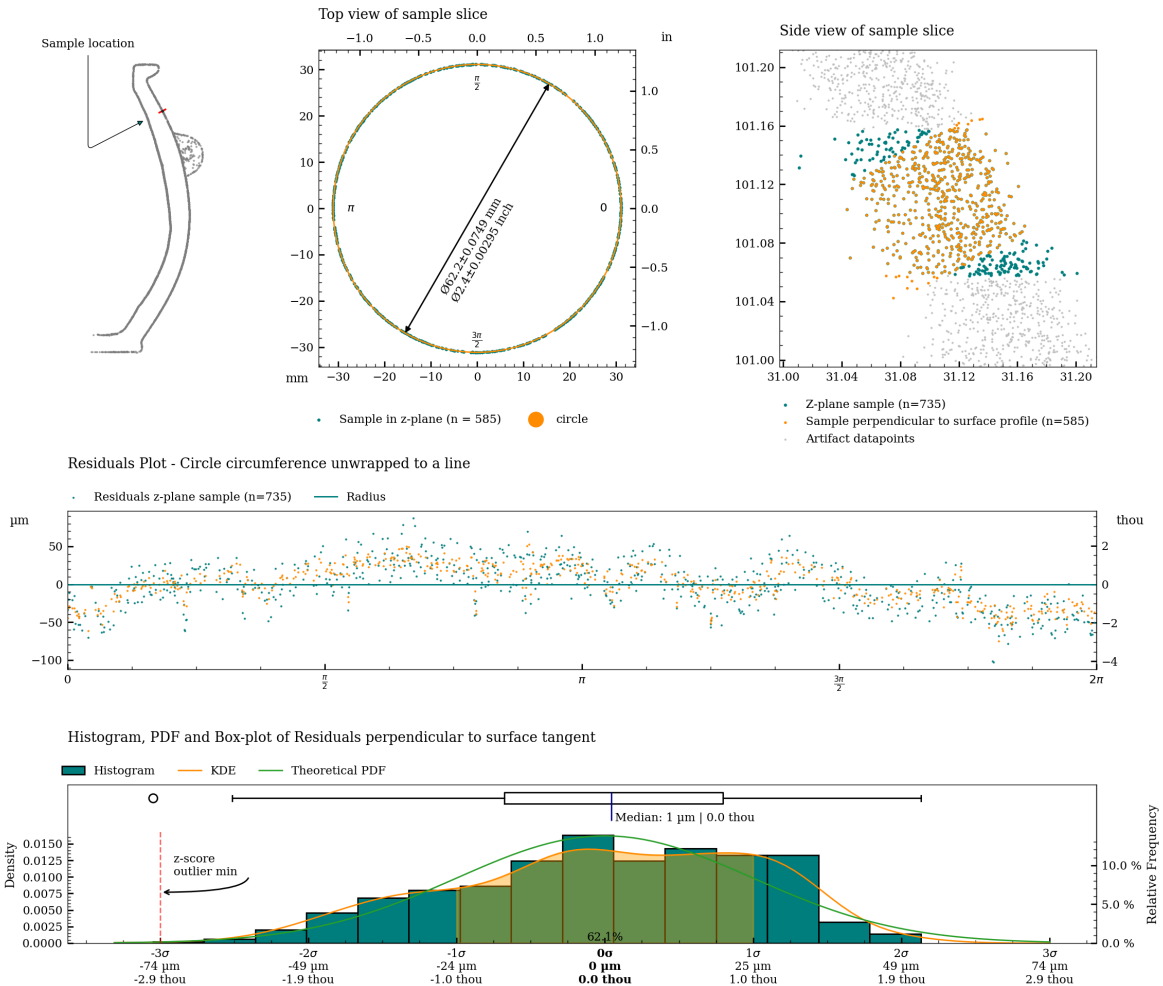


Figure 6: Charts with statistics for the measurement c02.

Graphical overview of circularity measurement c03

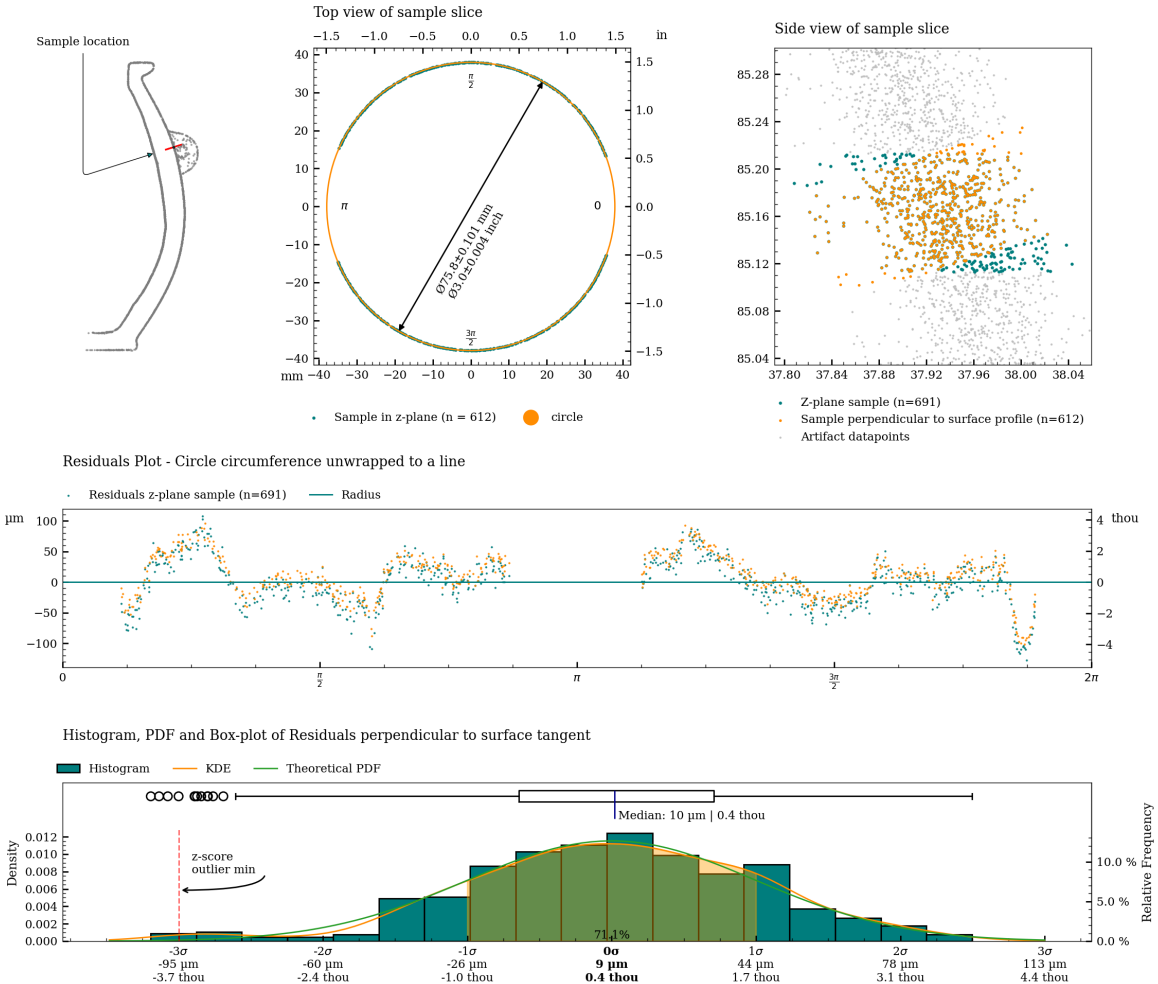


Figure 7: Charts with statistics for the measurement of c03.

Graphical overview of circularity measurement c04

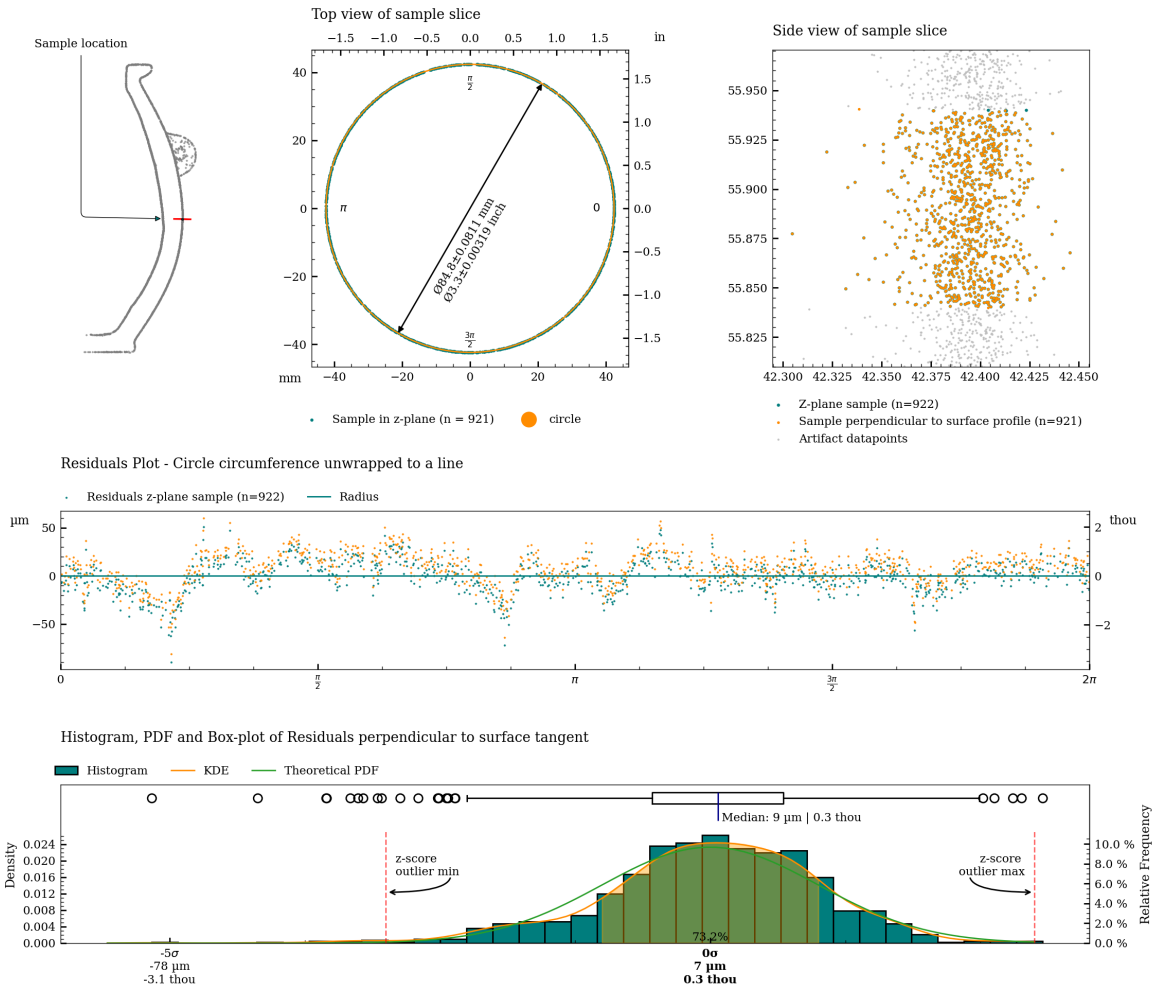


Figure 8: Charts with statistics for the measurement of c04.

Graphical overview of circularity measurement c05

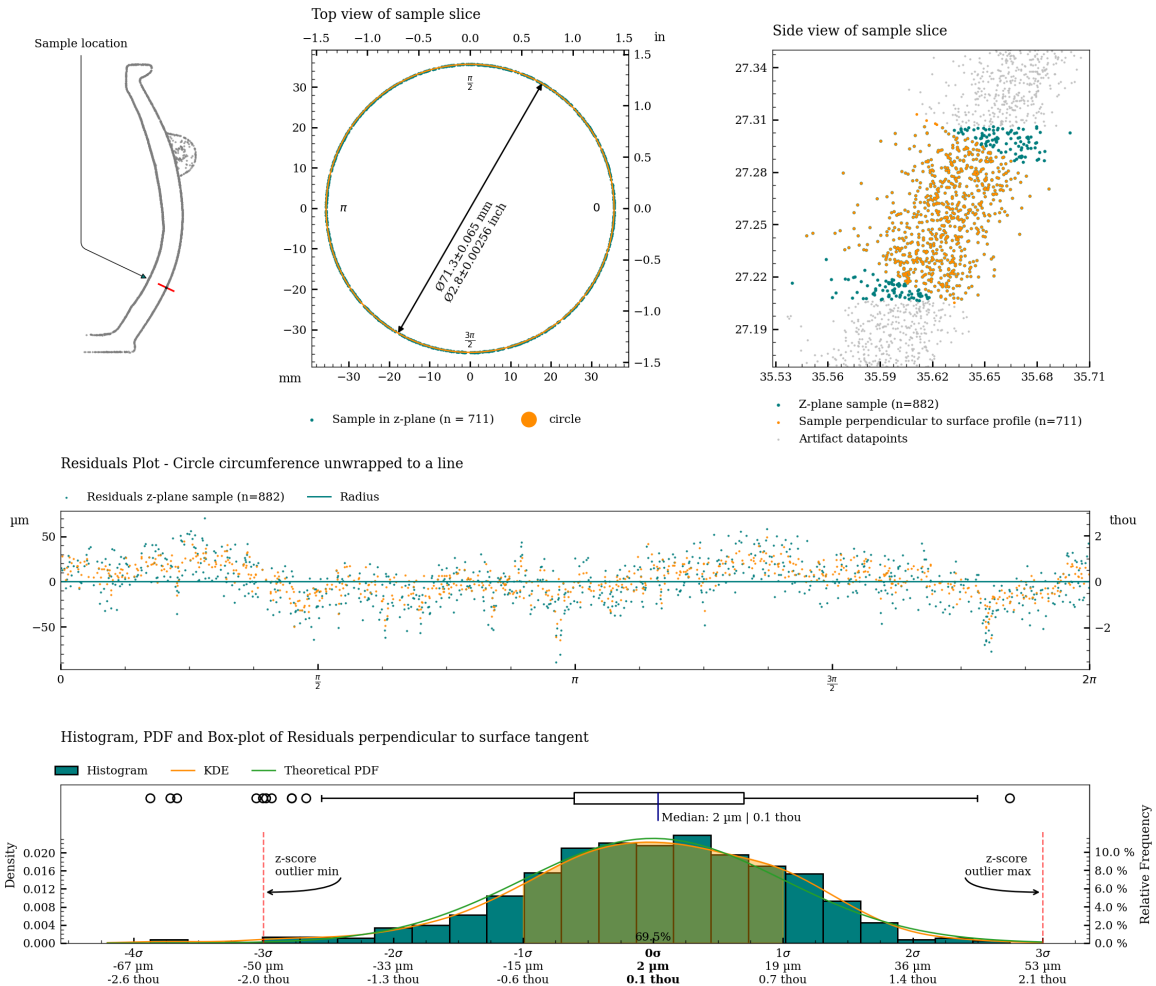


Figure 9: Charts with statistics for the measurement of c05.

Graphical overview of circularity measurement c06

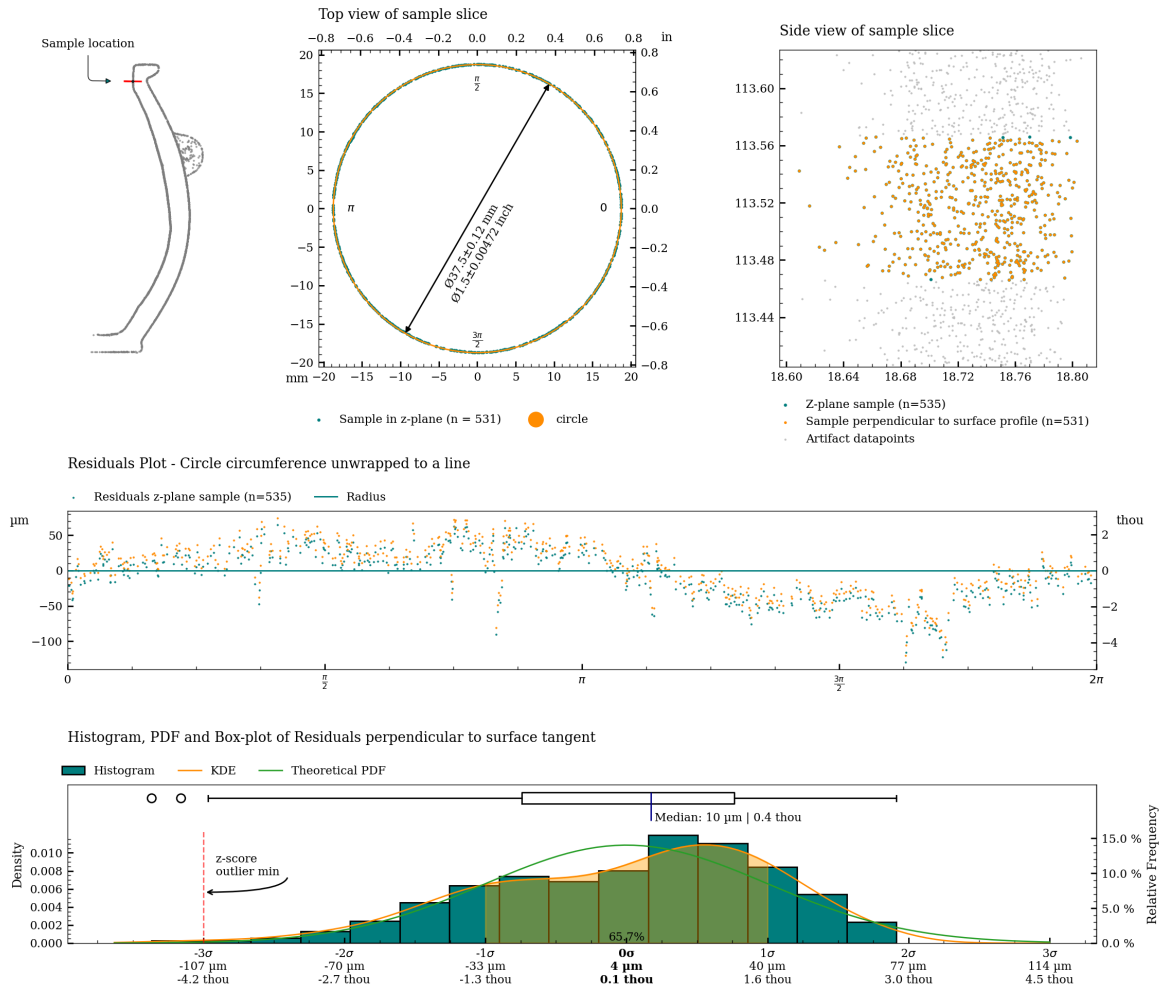


Figure 10: Charts with statistics for the measurement of c06.

Graphical overview of circularity measurement c07

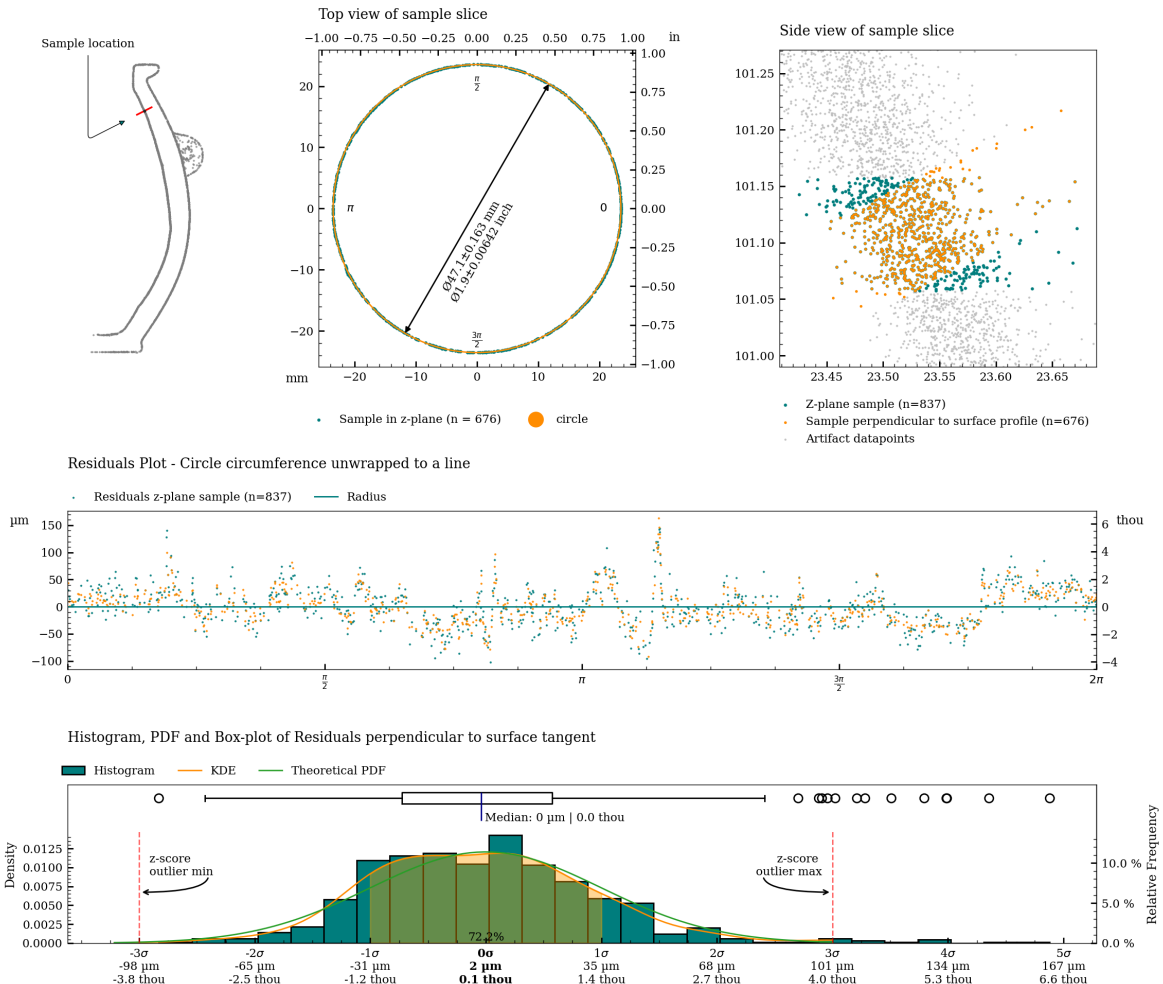


Figure 11: Charts with statistics for the measurement of c07.

Graphical overview of circularity measurement c08

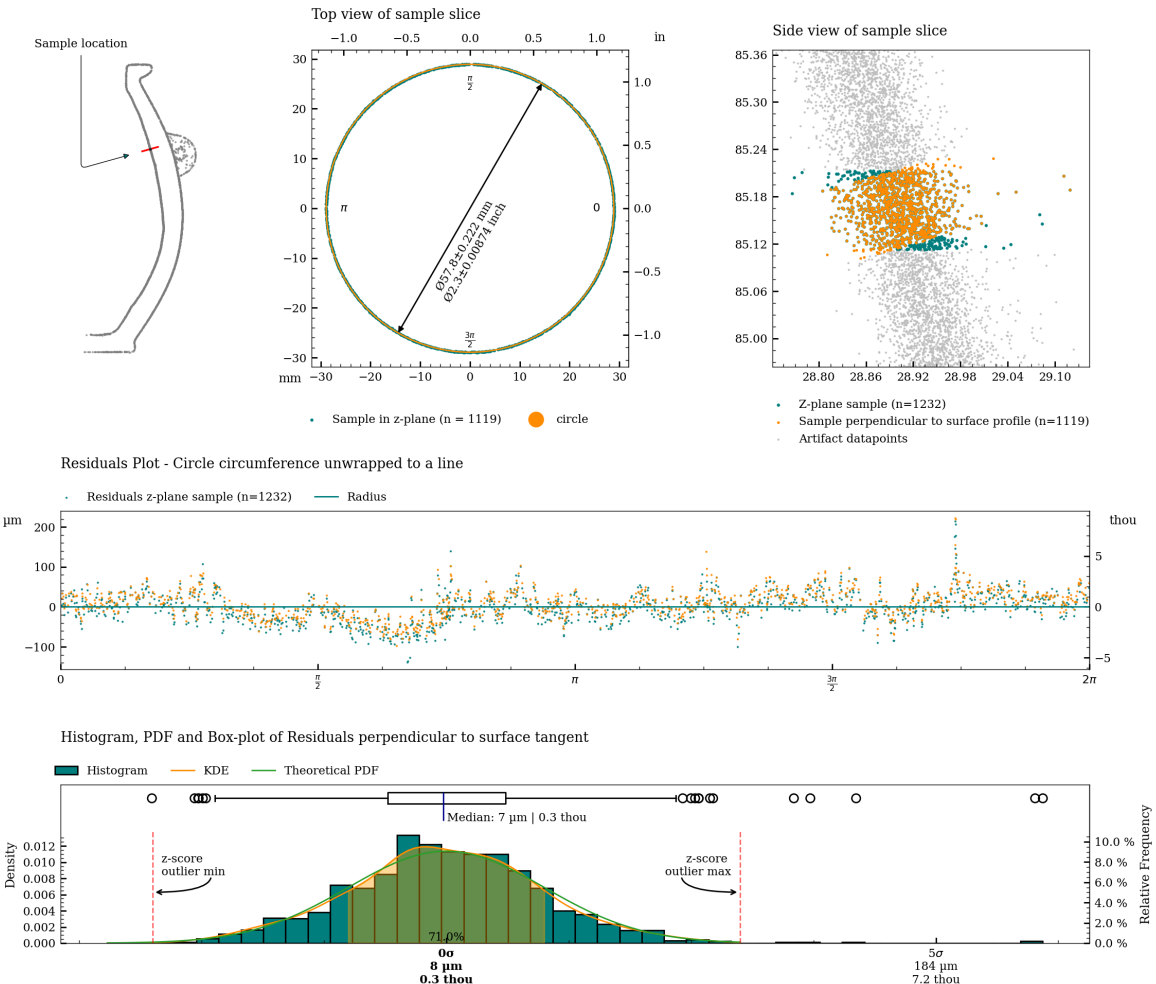


Figure 12: Charts with statistics for the measurement of c08.

Graphical overview of circularity measurement c09

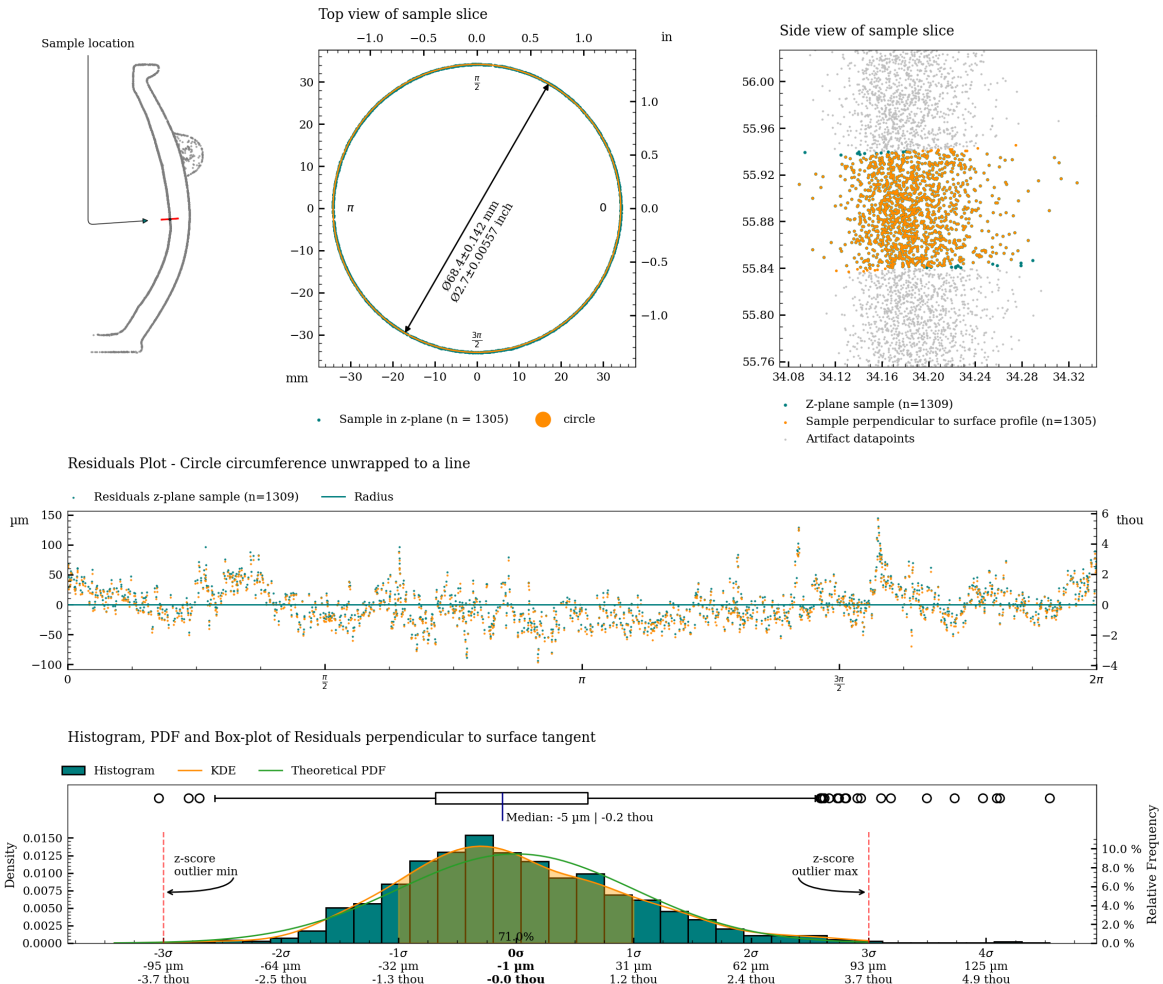


Figure 13: Charts with statistics for the measurement of c09.

Graphical overview of circularity measurement c10

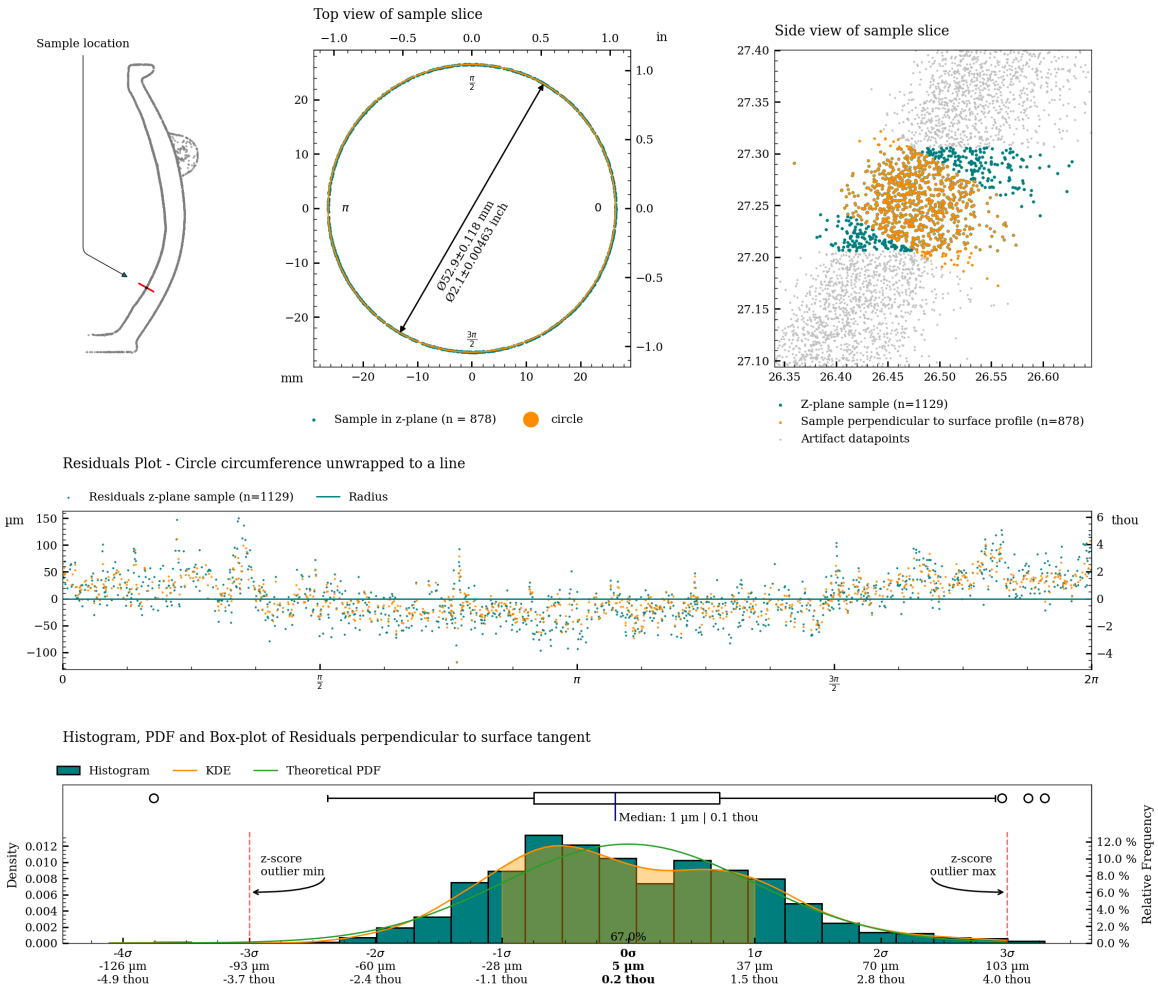


Figure 14: Charts with statistics for the measurement of c10.

Table 2 shows statistical measures of the circularity of the vessel, measured along the full height (damaged parts may reduce the measurement area).

Metric

Area	Range			Standard Deviation			Median Absolute Deviation			Slices	Slice height
	Median	Min.	Max.	Median	Min.	Max.	Median	Min.	Max.		
	mm	mm	mm	mm	mm	mm	mm	mm	mm		
Exterior	0.126	0.072	0.307	0.018	0.012	0.042	0.002	0.007	0.025	1190	0.100
Interior	0.235	0.103	0.800	0.033	0.019	0.081	0.002	0.011	0.036	1065	0.100

Imperial

Area	Range			Standard Deviation			Median Absolute Deviation			Slices	Slice height
	Median	Min.	Max.	Median	Min.	Max.	Median	Min.	Max.		
	in	in	in	in	in	in	in	in	in		
Exterior	0.126	0.072	0.307	0.018	0.012	0.042	0.002	0.007	0.025	1190	0.100
Interior	0.235	0.103	0.800	0.033	0.019	0.081	0.002	0.011	0.036	1065	0.100

Table 2: Perpendicular Circularity analysis of PV001.

Circularity analysis of exterior surface

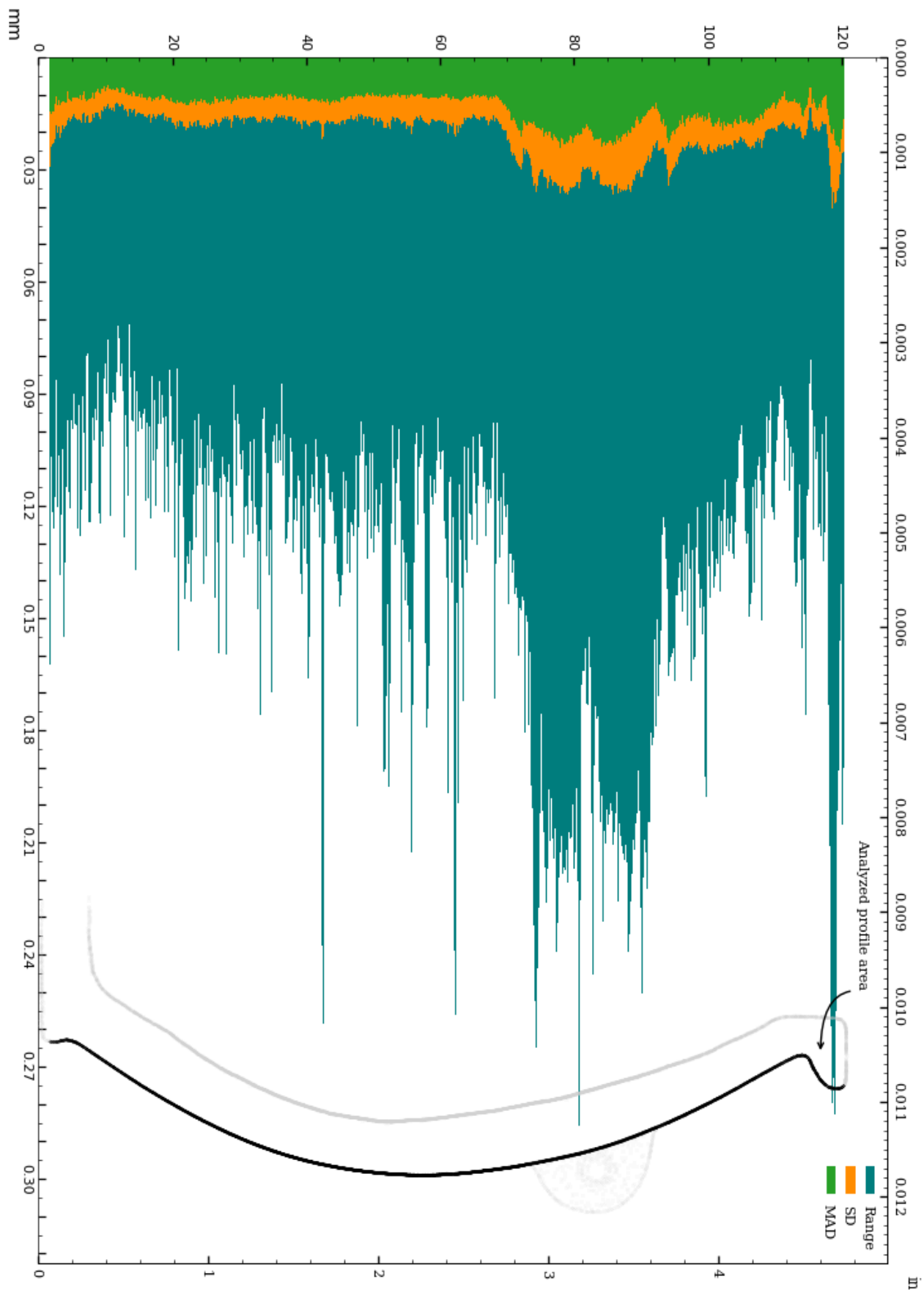


Figure 15: Circularity of exterior surface.

Circularity analysis of exterior surface, Standard Deviation and Median Absolute Deviation

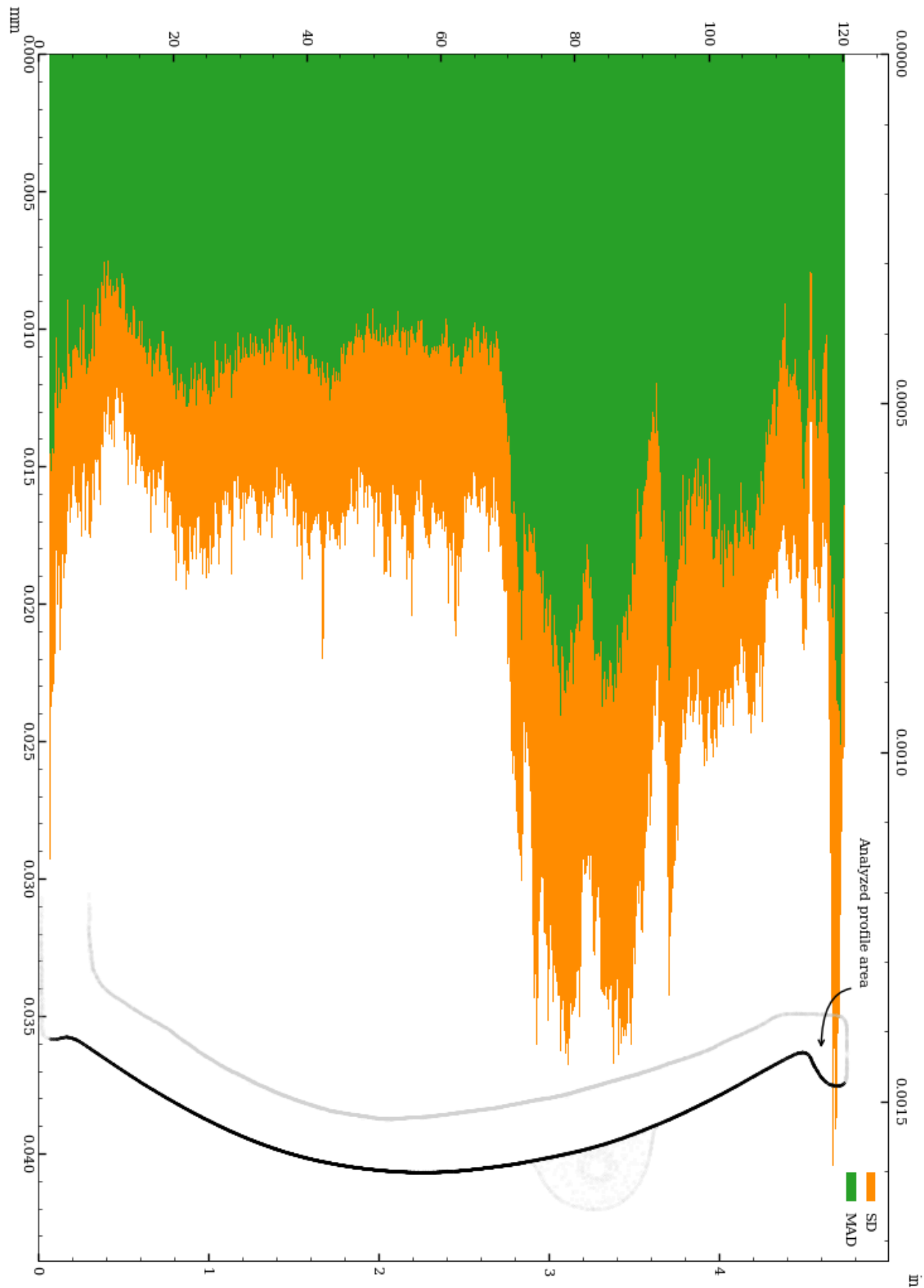


Figure 16: Vessel circularity of exterior surface, standard deviation and median absolute deviation.

The distributions of the circularity measurements across 1190 slices of the exterior surface are shown below.

Range measurement distribution across 1190 slices of exterior surface

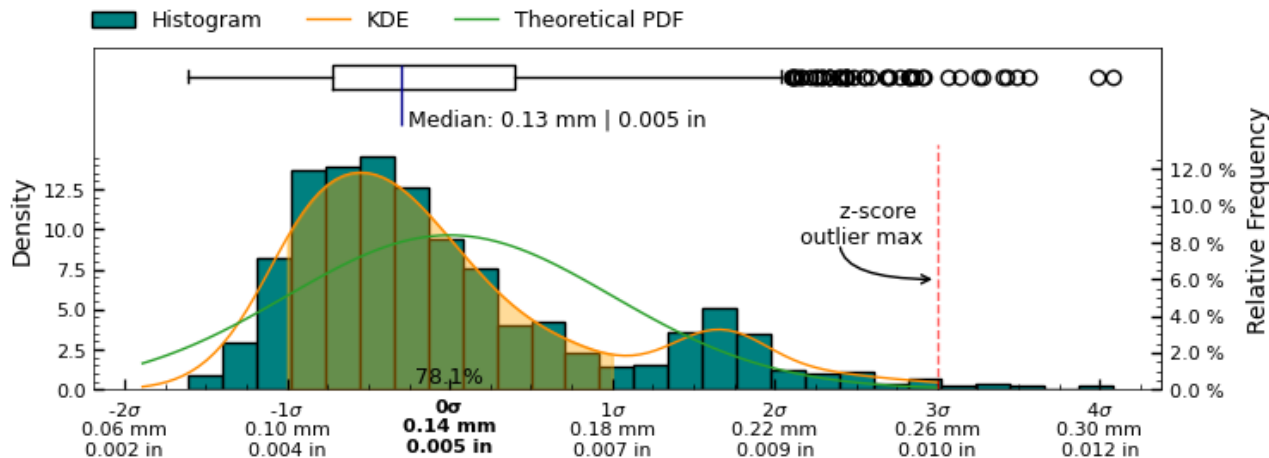


Figure 17: Range measurement distribution across measured slices of exterior surface

Standard deviation measurement distribution across 1190 slices of exterior surface

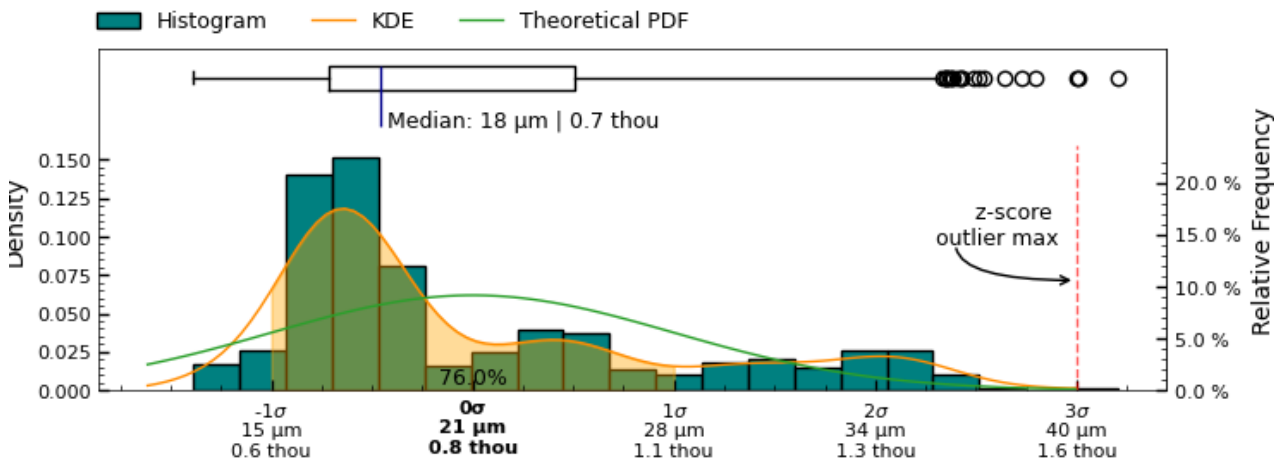


Figure 18: Standard deviation measurement distribution across measured slices of “+ exterior +” surface

Median absolute deviation measurement distribution across 1190 slices of exterior surface

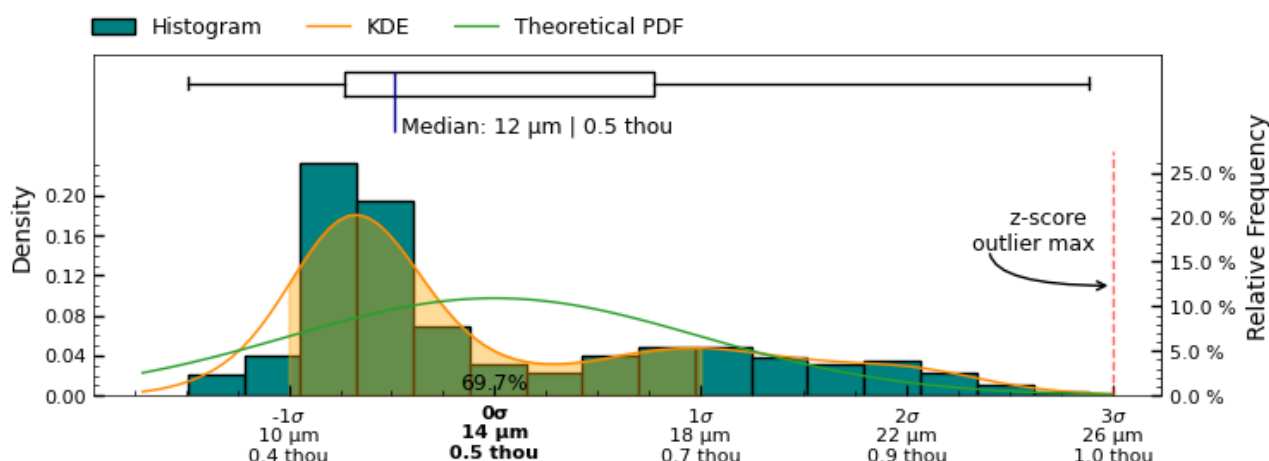


Figure 19: Median absolute deviation measurement distribution across measured slices of exterior surface

Circularity analysis of interior surface

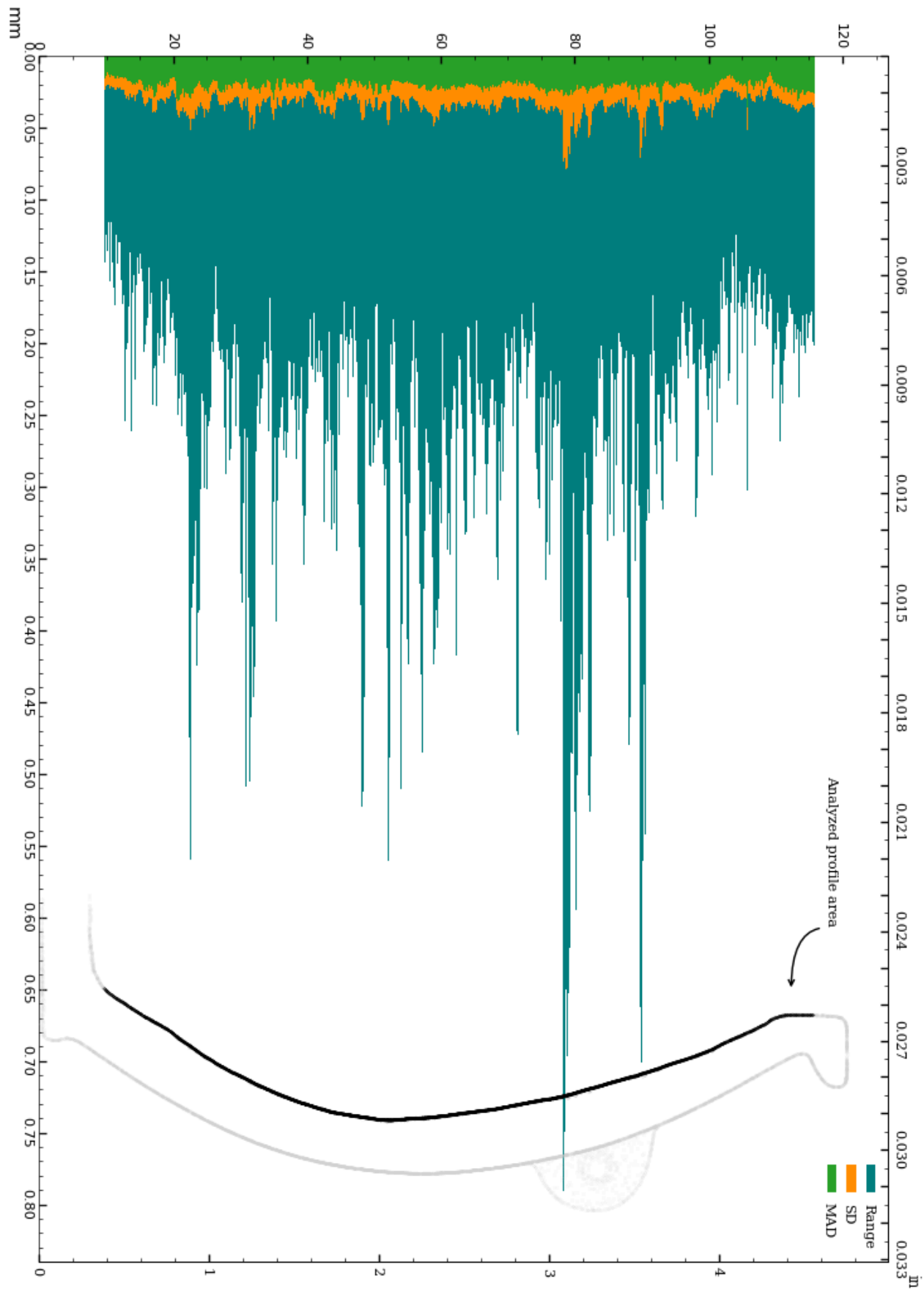


Figure 20: Circularity of interior surface.

Circularity analysis of interior surface, Standard Deviation and Median Absolute Deviation

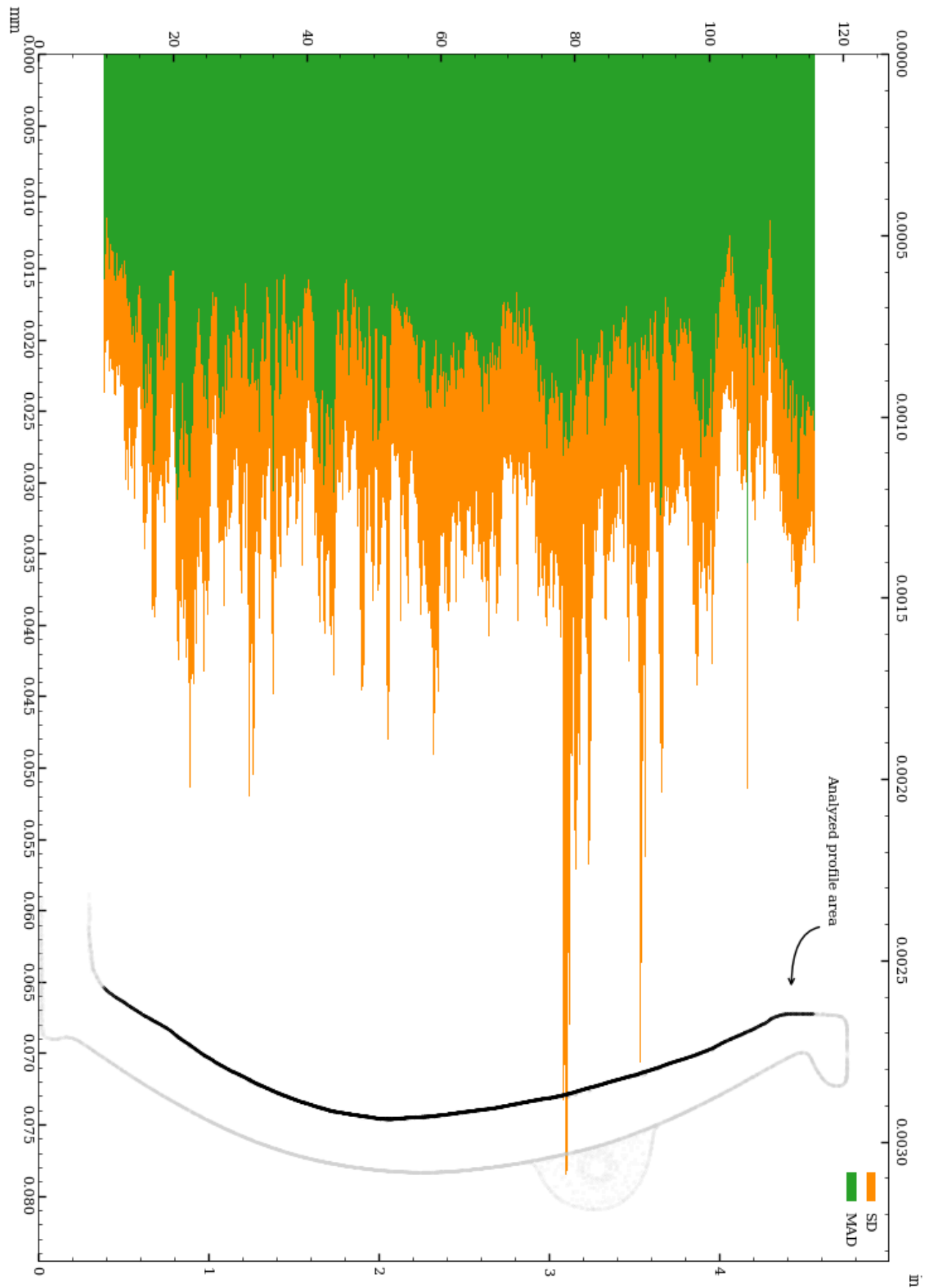
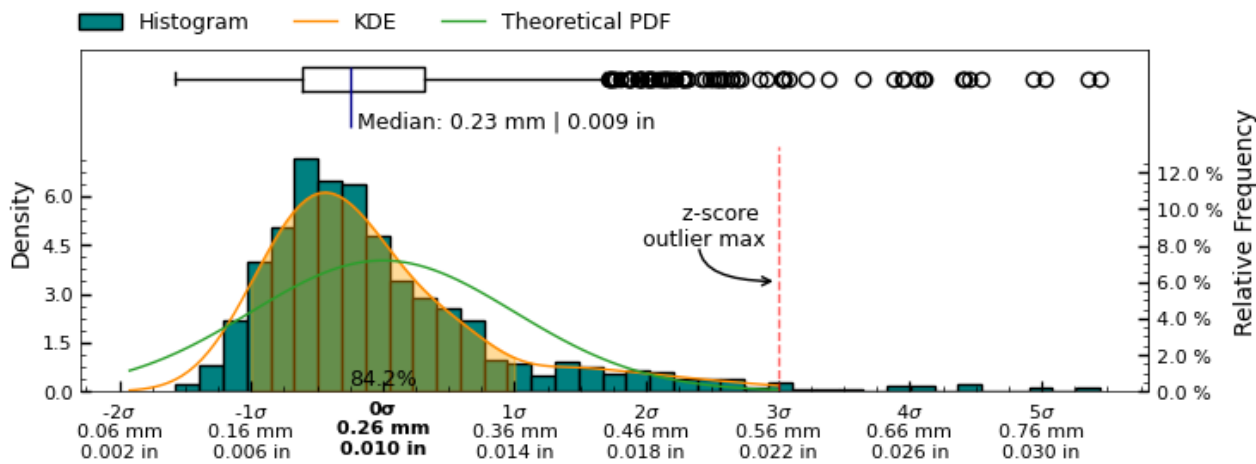


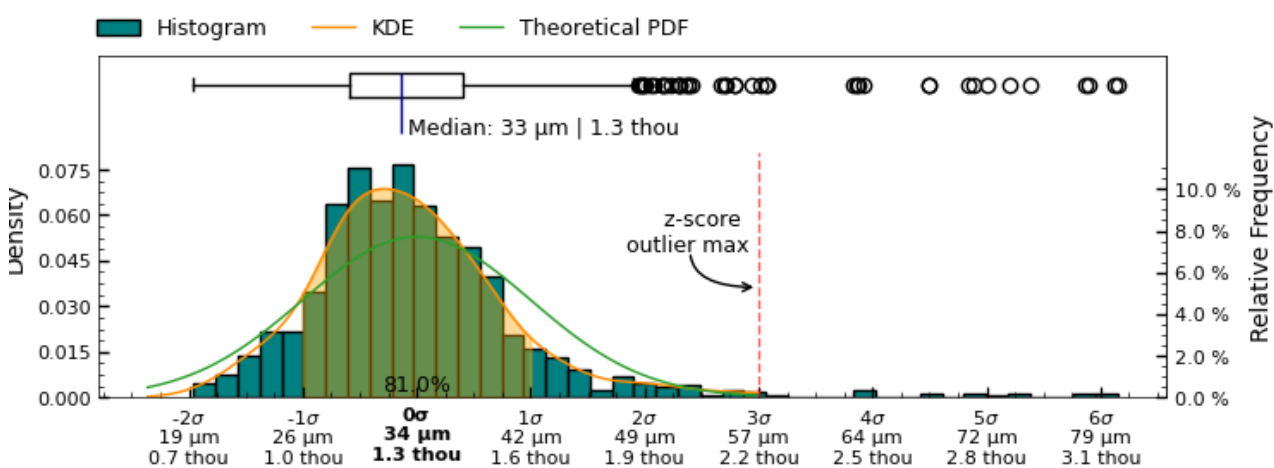
Figure 21: Vessel circularity of interior surface, standard deviation and median absolute deviation.

The distributions of the circularity measurements across 1065 slices of the interior surface are shown below.

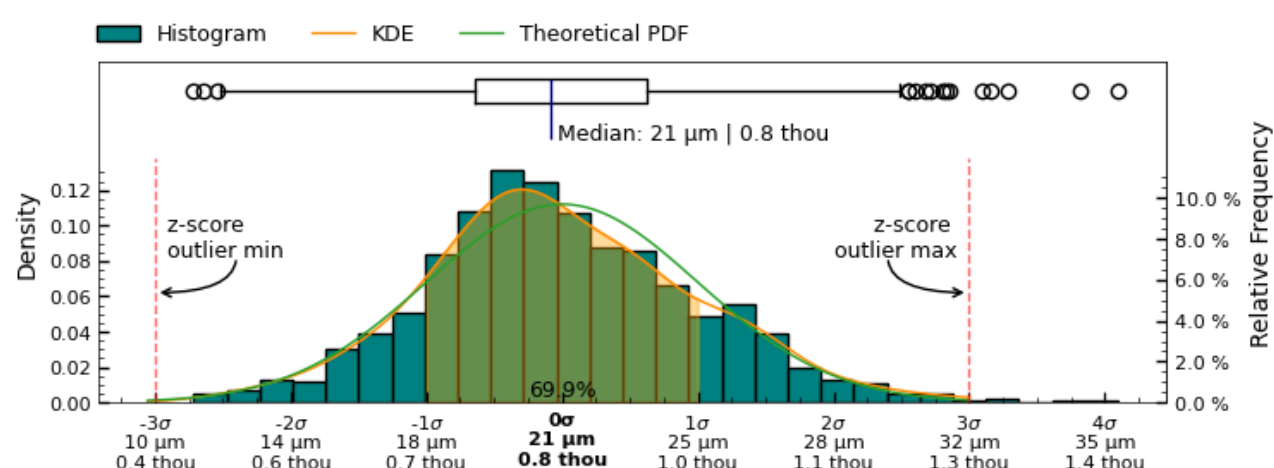
Range measurement distribution across 1065 slices of interior surface



Standard deviation measurement distribution across 1065 slices of interior surface



Median absolute deviation measurement distribution across 1065 slices of interior surface



Concentricity

The concentricity metric describes the deviation in the center-point of the referenced features. As such, it is a measure to determine if several features of the object share the same center point/axis, and how closely. See Figure 25 for a visual representation of this metric.

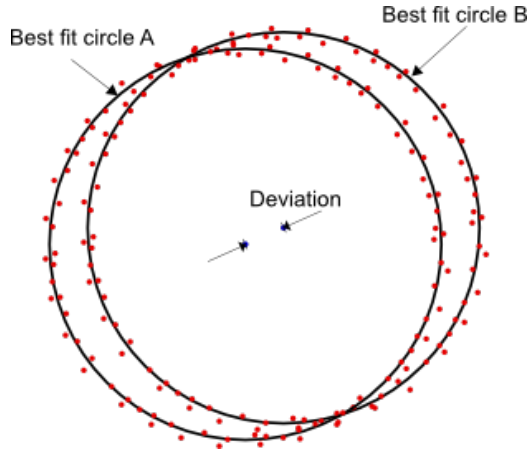


Figure 25: Concentricity measures the deviation (distance) between the center of two circles.

Determination of concentricity has been carried out by establishing the best fit circles of sample slices, using RANSAC (Random sample consensus) algorithm for outlier detection of a least squares circle regression on the scanned data-points at each cross-section, to estimate centers of each cross-section.

The concentricity between both the interior and exterior circular cross-sections is explored for cross-section measurements with the same Z-coordinates.

Additionally, the concentricity between each cross-section measurement defined in Figure 4 and the datum axis $(x, y) = (0, 0)$ has been calculated to establish the deviation of the feature center from the datum axis.

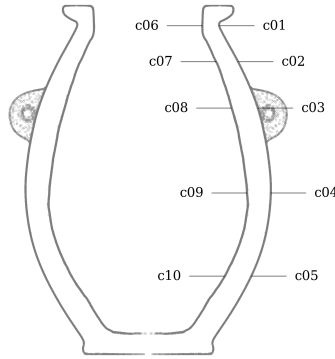


Figure 26: Concentricity measurement sample location on PV001.

Metric

Tag	Reference	Deviation	Sample size	Circle fit residuals analysis for sample listed in Tag column						
				Range full	Range inliers	SD full	SD inliers	MAD full	MAD inliers	Center (x,y)
				mm	mm	mm	mm	mm	mm	μm
c01	z-axis	0.011	473	0.114	0.085	0.019	0.018	0.012	0.012	-6, 9
c02	z-axis	0.023	585	0.128	0.128	0.025	0.024	0.019	0.018	-19, 13
c03	z-axis	0.012	612	0.197	0.186	0.035	0.033	0.023	0.023	-12, 2
c04	z-axis	0.004	921	0.141	0.078	0.017	0.015	0.010	0.010	-2, 3
c05	z-axis	0.005	711	0.114	0.095	0.017	0.016	0.011	0.011	3, -4
c06	z-axis	0.042	531	0.194	0.159	0.037	0.035	0.027	0.025	-12, 40
c07	z-axis	0.011	676	0.255	0.191	0.033	0.029	0.021	0.021	10, 4
c08	z-axis	0.023	1119	0.319	0.196	0.035	0.032	0.021	0.021	11, -20
c09	z-axis	0.019	1305	0.238	0.173	0.031	0.029	0.020	0.020	19, -1
c10	z-axis	0.028	878	0.230	0.185	0.033	0.031	0.023	0.023	27, -5
c01	c06	0.032	473	0.114	0.085	0.019	0.018	0.012	0.012	5, -32
c02	c07	0.030	585	0.128	0.128	0.025	0.024	0.019	0.018	-29, 9
c03	c08	0.032	612	0.197	0.186	0.035	0.033	0.023	0.023	-23, 22
c04	c09	0.021	921	0.141	0.078	0.017	0.015	0.010	0.010	-21, 4
c05	c10	0.025	711	0.114	0.095	0.017	0.016	0.011	0.011	-25, 0

Imperial

Tag	Reference	Deviation	Sample size	Circle fit residuals analysis for sample listed in Tag column						
				Range full	Range inliers	SD full	SD inliers	MAD full	MAD inliers	Center (x,y)
				in	in	in	in	in	in	thou
c01	z-axis	0.0004	473	0.0045	0.0033	0.0007	0.0007	0.0005	0.0005	-0.2, 0.3
c02	z-axis	0.0009	585	0.0050	0.0050	0.0010	0.0010	0.0007	0.0007	-0.7, 0.5
c03	z-axis	0.0005	612	0.0078	0.0073	0.0014	0.0013	0.0009	0.0009	-0.5, 0.1
c04	z-axis	0.0001	921	0.0056	0.0031	0.0007	0.0006	0.0004	0.0004	-0.1, 0.1
c05	z-axis	0.0002	711	0.0045	0.0037	0.0007	0.0006	0.0004	0.0004	0.1, -0.2
c06	z-axis	0.0017	531	0.0076	0.0063	0.0014	0.0014	0.0010	0.0010	-0.5, 1.6
c07	z-axis	0.0004	676	0.0100	0.0075	0.0013	0.0012	0.0008	0.0008	0.4, 0.2
c08	z-axis	0.0009	1119	0.0126	0.0077	0.0014	0.0013	0.0008	0.0008	0.4, -0.8
c09	z-axis	0.0008	1305	0.0094	0.0068	0.0012	0.0011	0.0008	0.0008	0.8, -0.0
c10	z-axis	0.0011	878	0.0090	0.0073	0.0013	0.0012	0.0009	0.0009	1.1, -0.2
c01	c06	0.0013	473	0.0045	0.0033	0.0007	0.0007	0.0005	0.0005	0.2, -1.3
c02	c07	0.0012	585	0.0050	0.0050	0.0010	0.0010	0.0007	0.0007	-1.1, 0.3
c03	c08	0.0013	612	0.0078	0.0073	0.0014	0.0013	0.0009	0.0009	-0.9, 0.9
c04	c09	0.0008	921	0.0056	0.0031	0.0007	0.0006	0.0004	0.0004	-0.8, 0.2
c05	c10	0.0010	711	0.0045	0.0037	0.0007	0.0006	0.0004	0.0004	-1.0, 0.0

Table 3: Concentricity analysis of PV001.

Concentricity analysis of c01

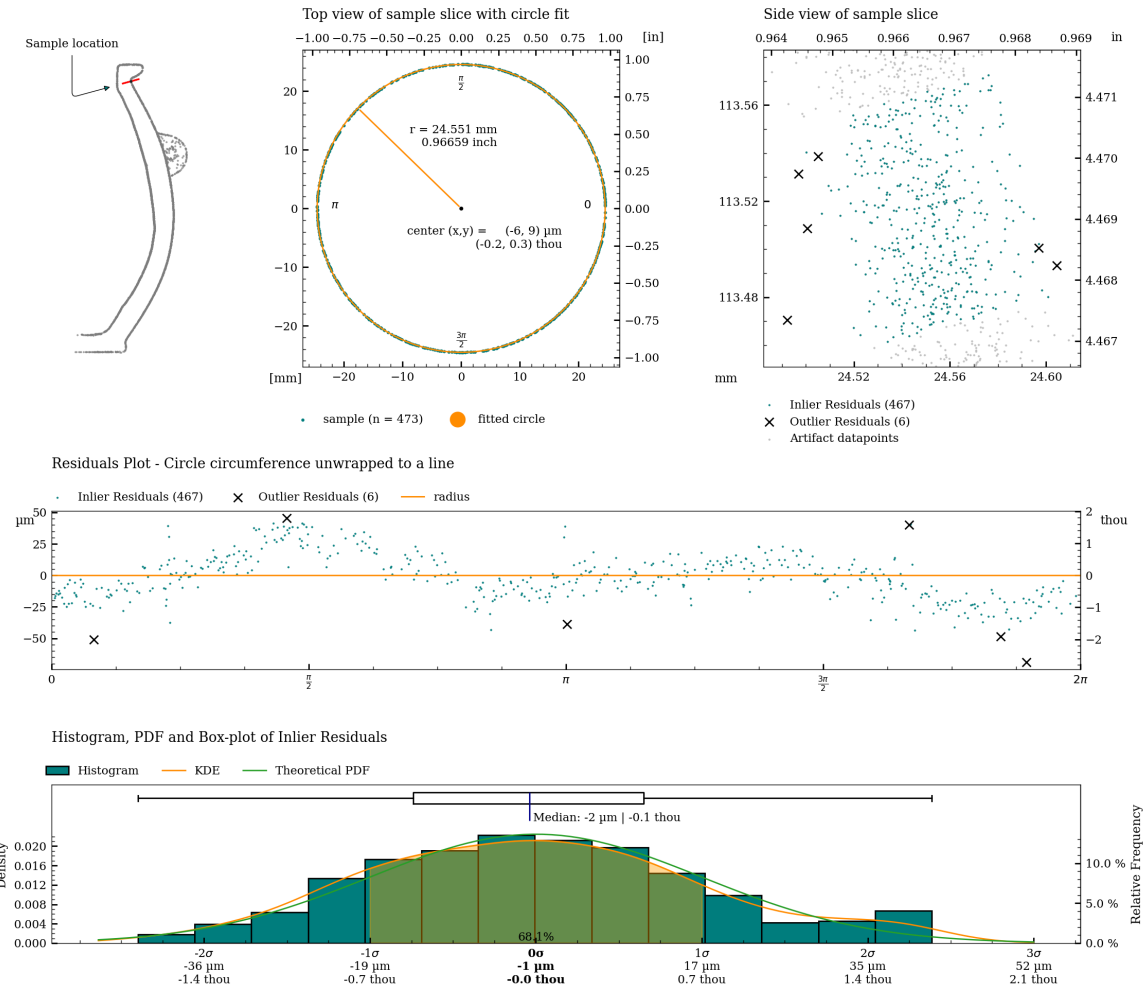


Figure 27: Detailed plot of concentricity measurement for c01.

Concentricity analysis of c02

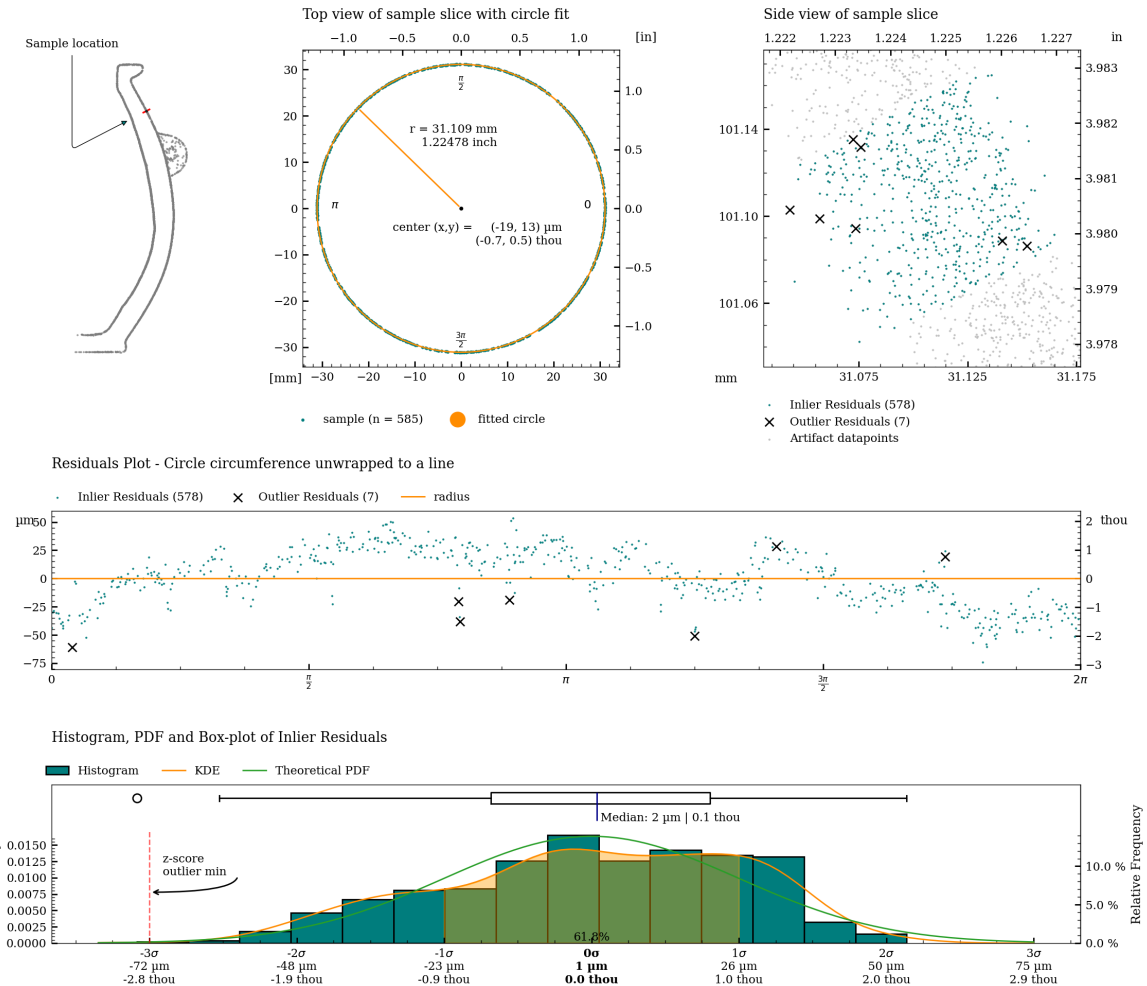


Figure 28: Detailed plot of concentricity measurement for c02.

Concentricity analysis of c03

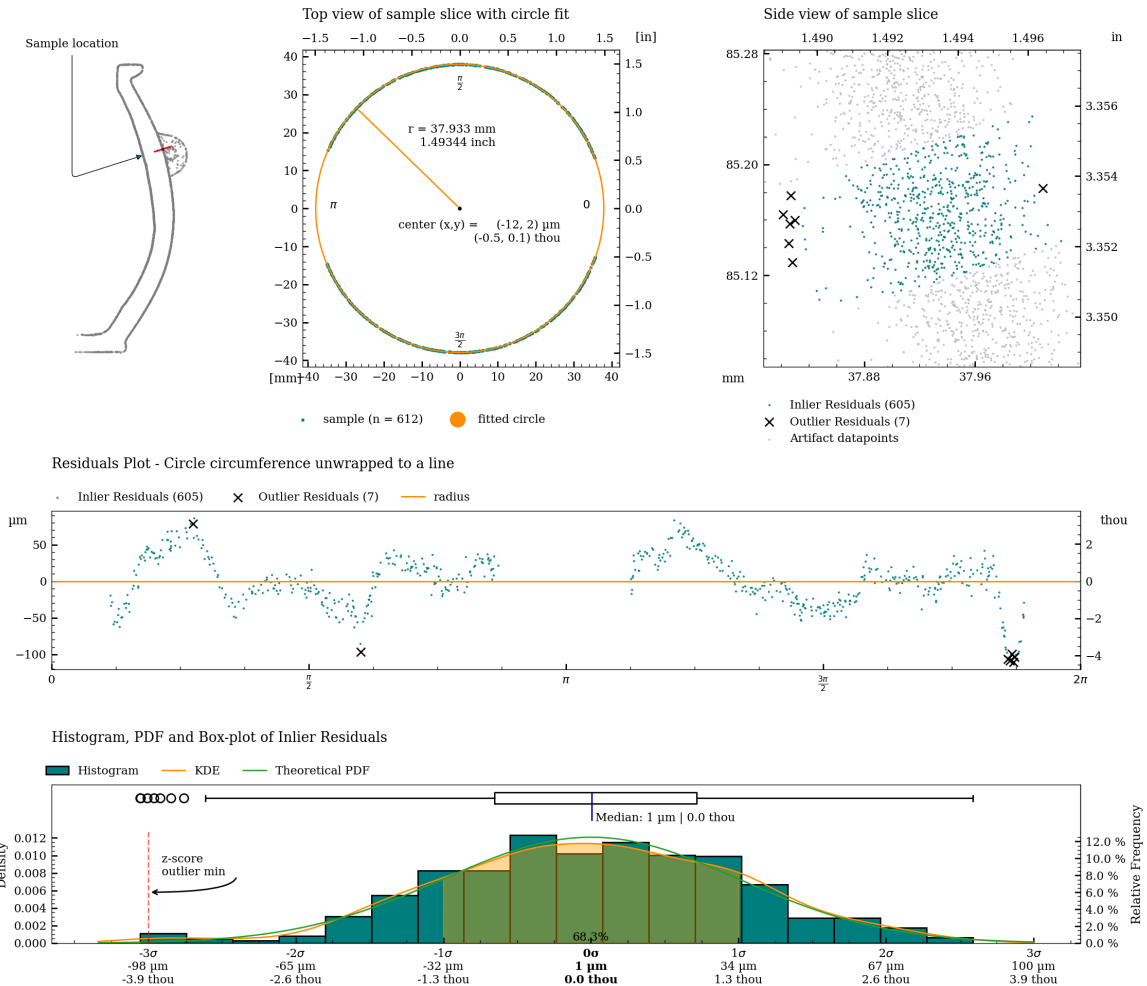


Figure 29: Detailed plot of concentricity measurement for c03.

Concentricity analysis of c04

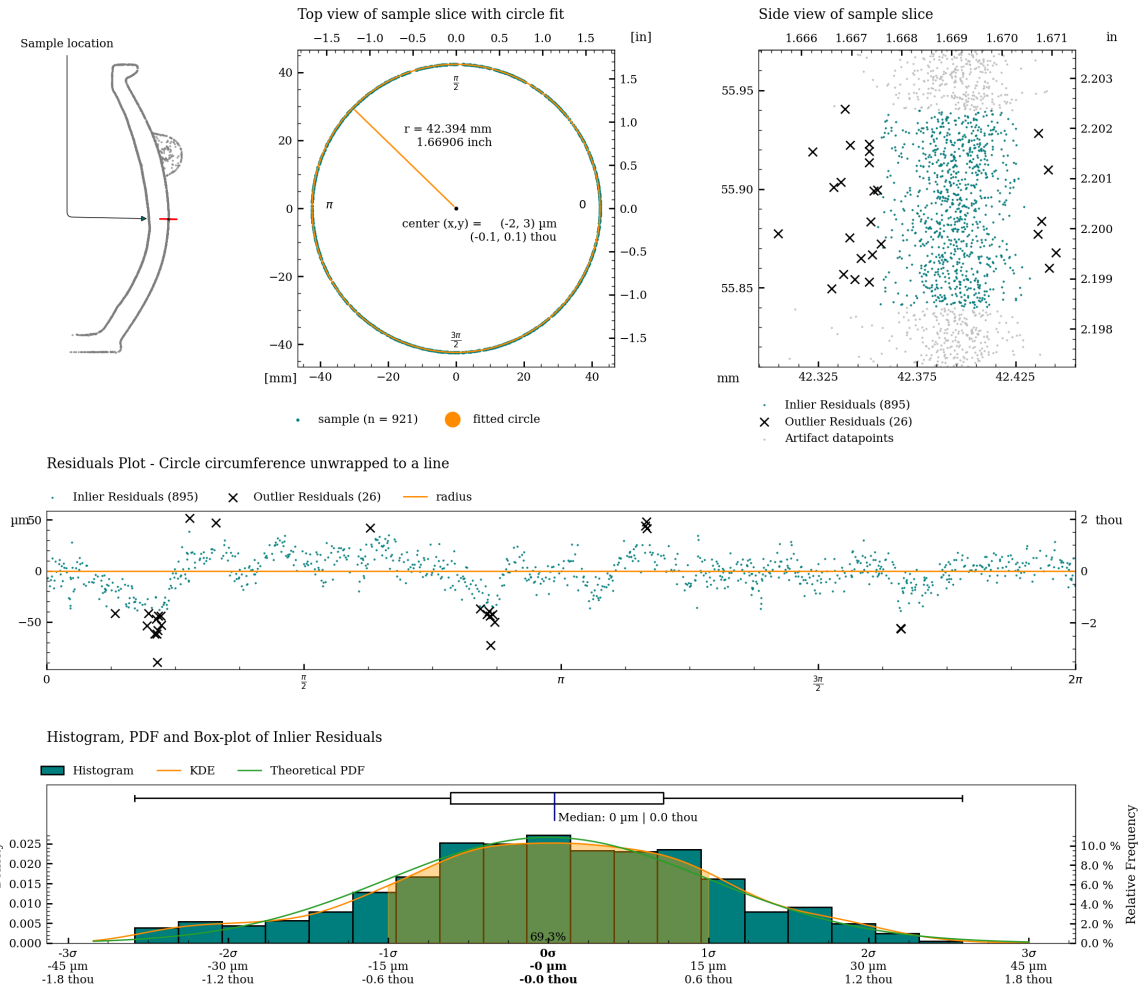


Figure 30: Detailed plot of concentricity measurement for c04.

Concentricity analysis of c05

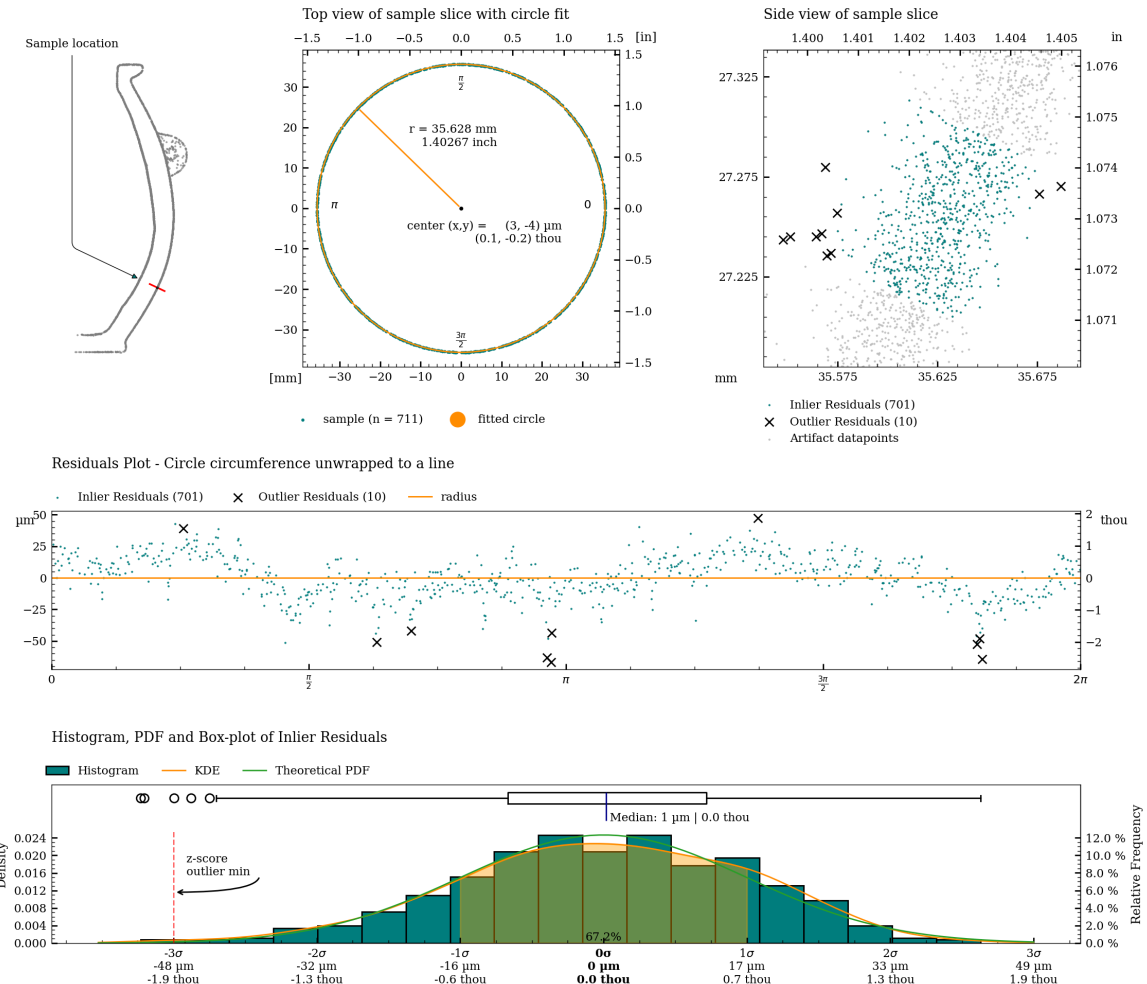


Figure 31: Detailed plot of concentricity measurement for c05.

Concentricity analysis of c06

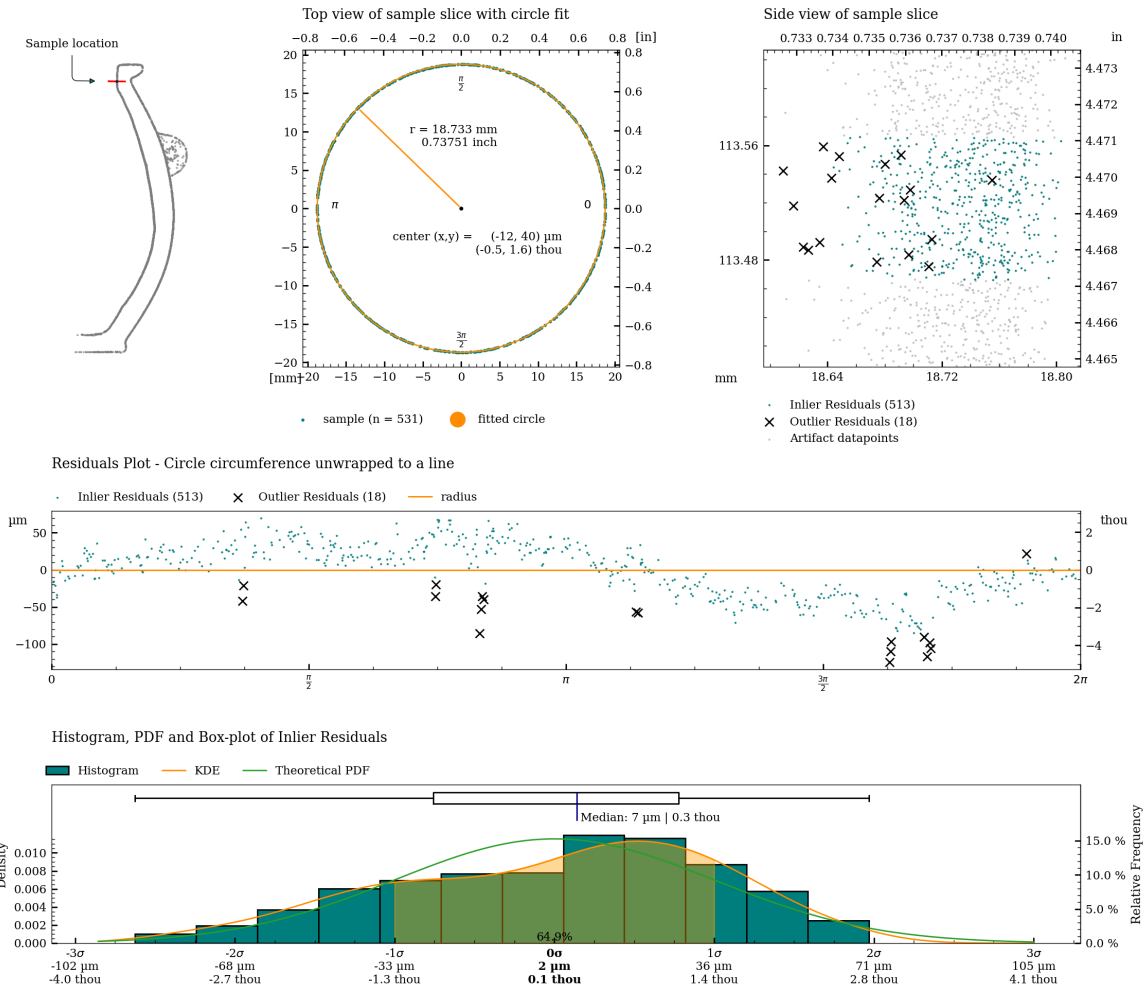


Figure 32: Detailed plot of concentricity measurement for c06.

Concentricity analysis of c07

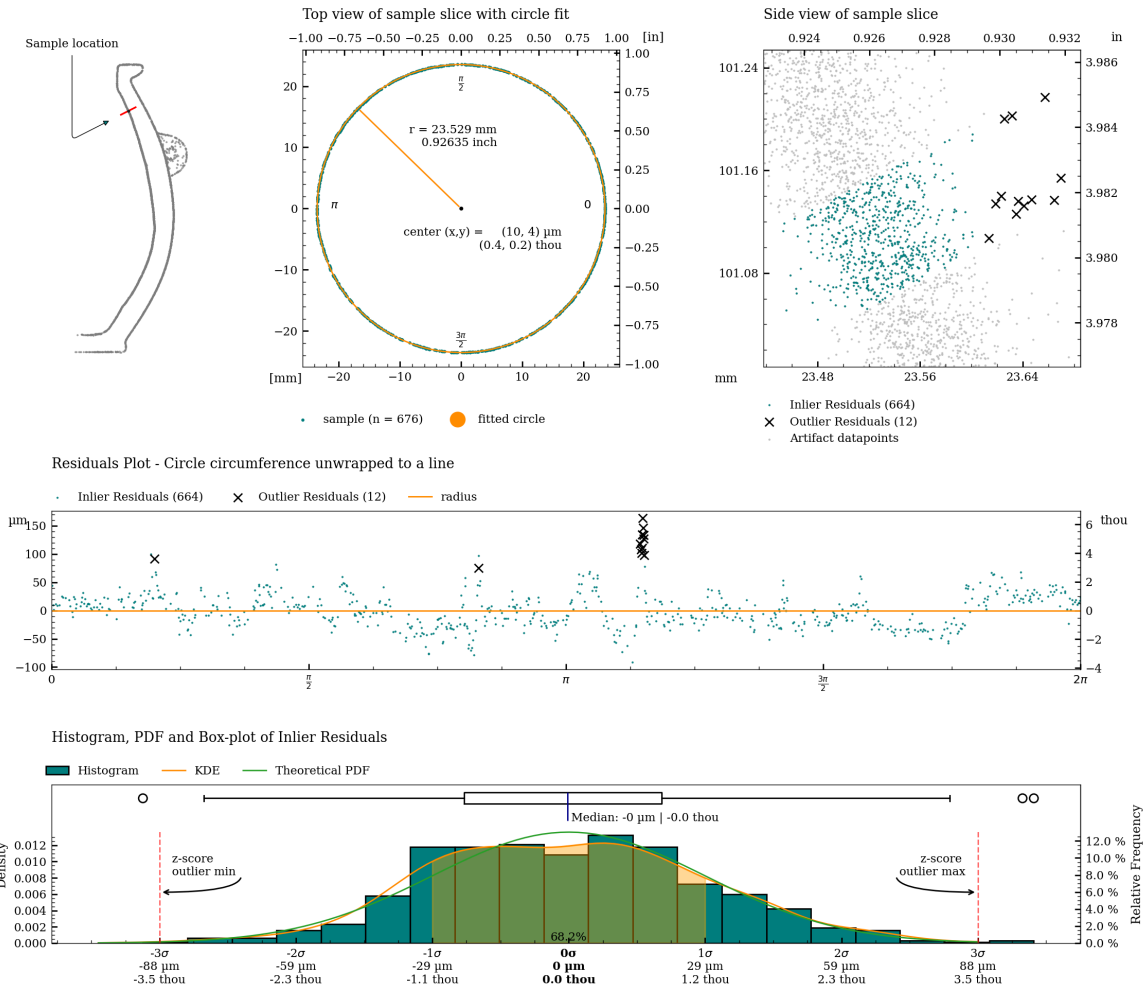


Figure 33: Detailed plot of concentricity measurement for c07.

Concentricity analysis of c08

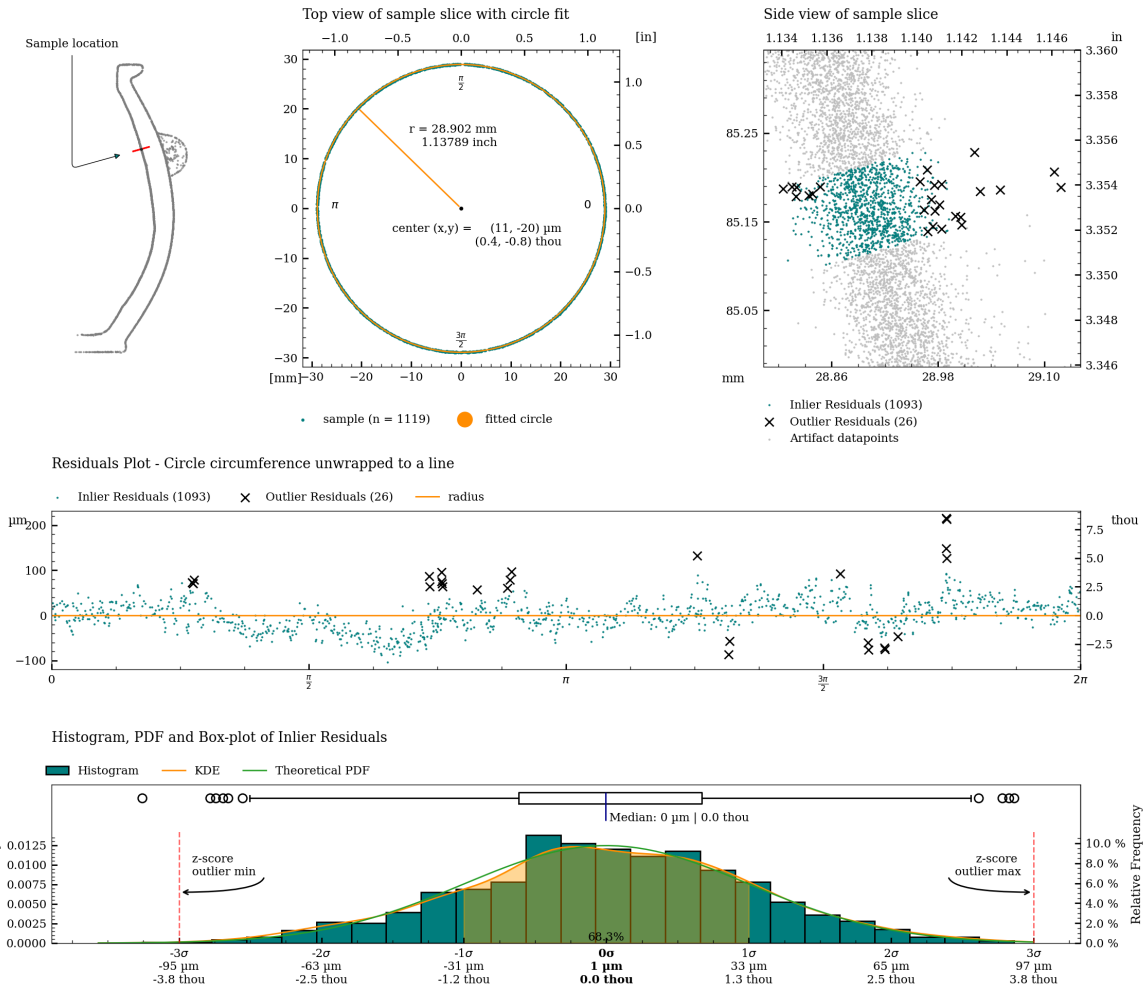


Figure 34: Detailed plot of concentricity measurement for c08.

Concentricity analysis of c09

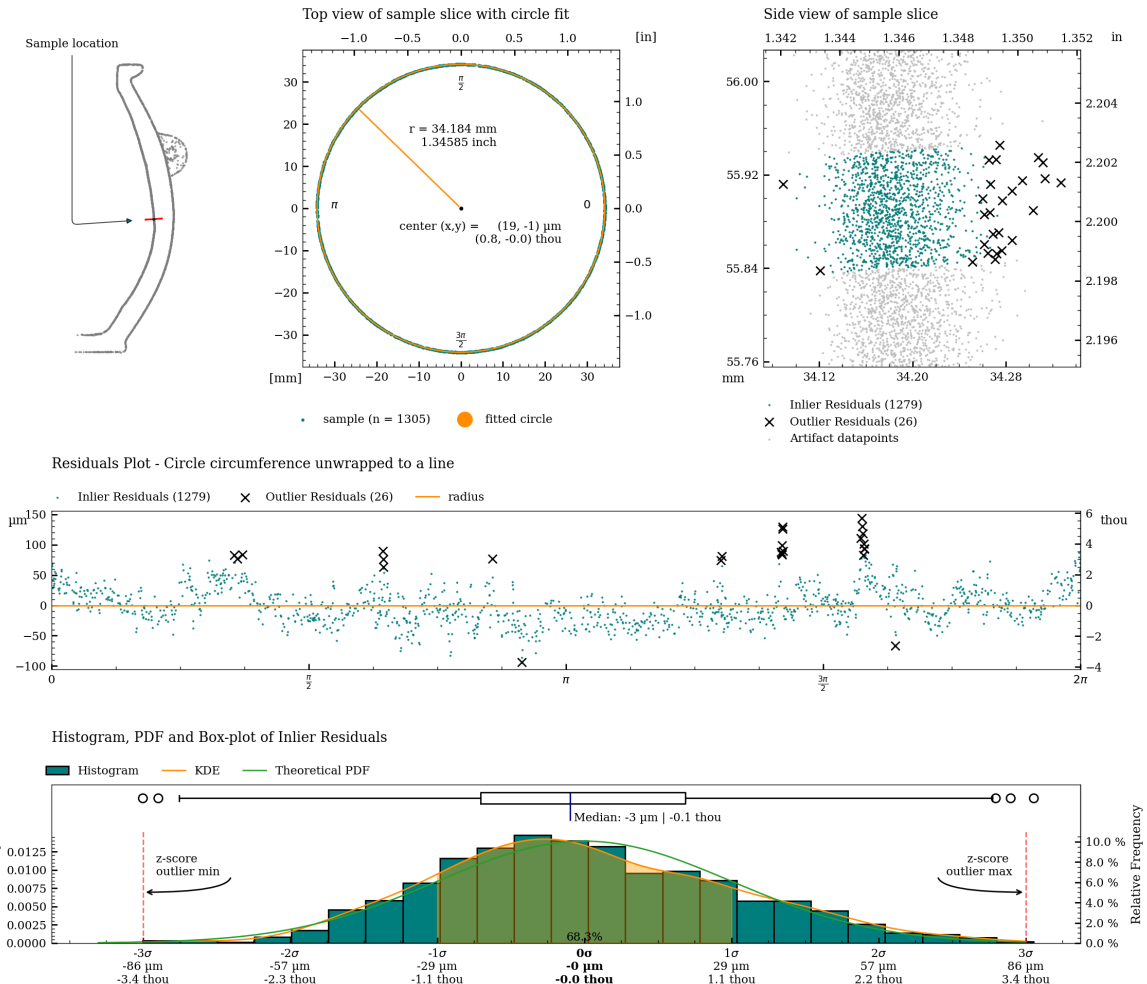


Figure 35: Detailed plot of concentricity measurement for c09.

Concentricity analysis of c10

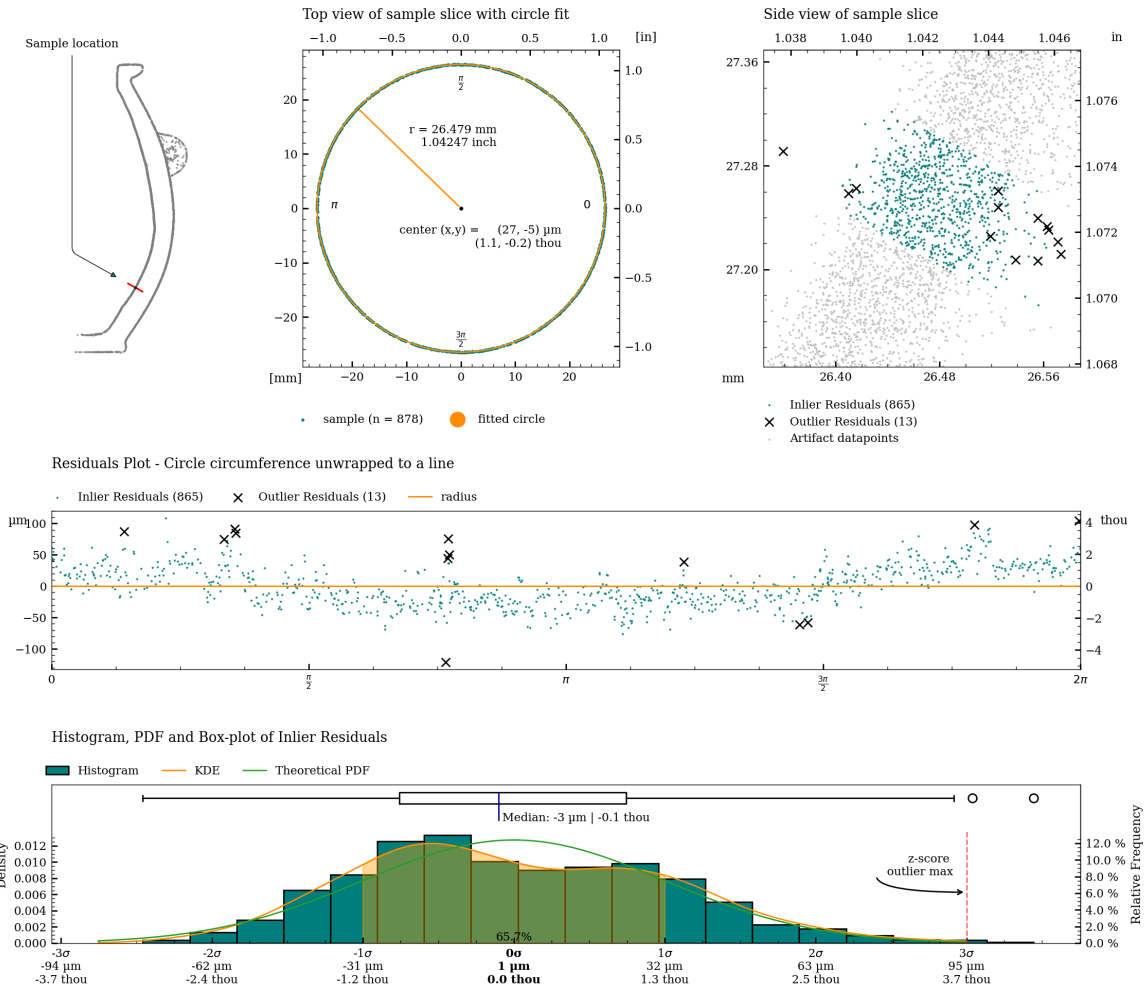


Figure 36: Detailed plot of concentricity measurement for c10.

Coaxiality

Coaxiality is a measure of the deviation in the central axis of an object. Coaxiality measurements are calculated using RANSAC (Random sample consensus) algorithm for outlier detection of a least squares circle regression on cross-sections of the vessel (excluding potential handles) to estimate the best fit circle centers for each slice of the vessel.

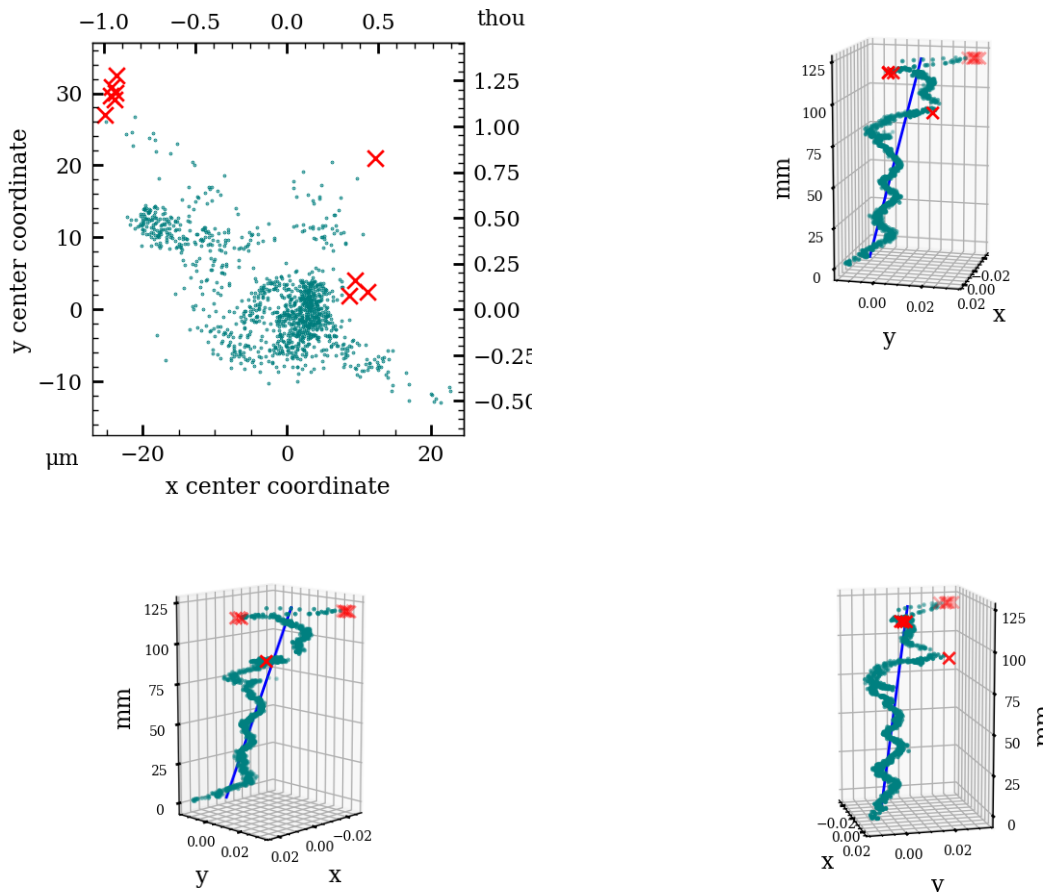
Coaxiality is measured for:

- The exterior surface (excluding handles)
- The interior surface

	Exterior	Interior	
Analyzed Slices	1190		1065
Median sample size	660		1076
Slice Height	100 µm	3.9 thou	100 µm
Statistics with Z-axis as Reference			
Median Absolute Deviation (MAD)	6 µm	0.2 thou	16 µm
Standard Deviation (SD)	7 µm	0.3 thou	9 µm
Root Mean Square Deviation (RMSD)	12 µm	0.5 thou	20 µm
Statistics with Best Fit Central Axis as Reference			
Best fit Central Axis Equation (in metric coordinate system with unit [mm])	$x = 0.009 + t - 0.00018$ $y = -0.007 + t0.00014$ $z = 0.000 + t1.00000$	$x = 0.017 + t - 0.00011$ $y = 0.001 + t0.00005$ $z = 0.000 + t1.00000$	
Axis tilt		-0.01°	-0.006°
Median Absolute Deviation (MAD)	5 µm	0.2 thou	13 µm
Standard Deviation (SD)	4 µm	0.2 thou	8 µm
Root Mean Square Deviation (RMSD)	8 µm	0.3 thou	16 µm

Table 4: Coaxiality analysis of vessel PV001.

Coaxiality plots, exterior surface



Coaxiality residuals from fitted axis, exterior surface

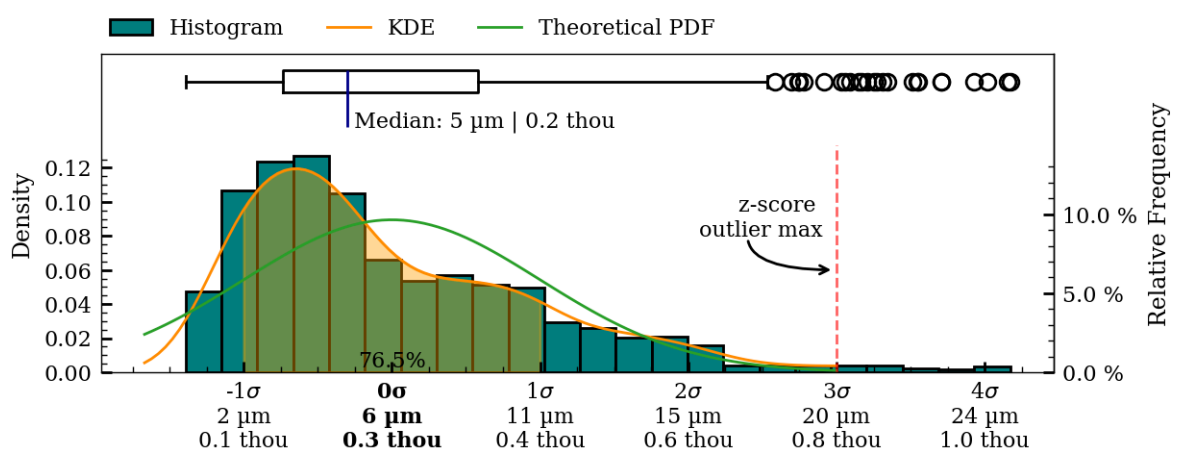
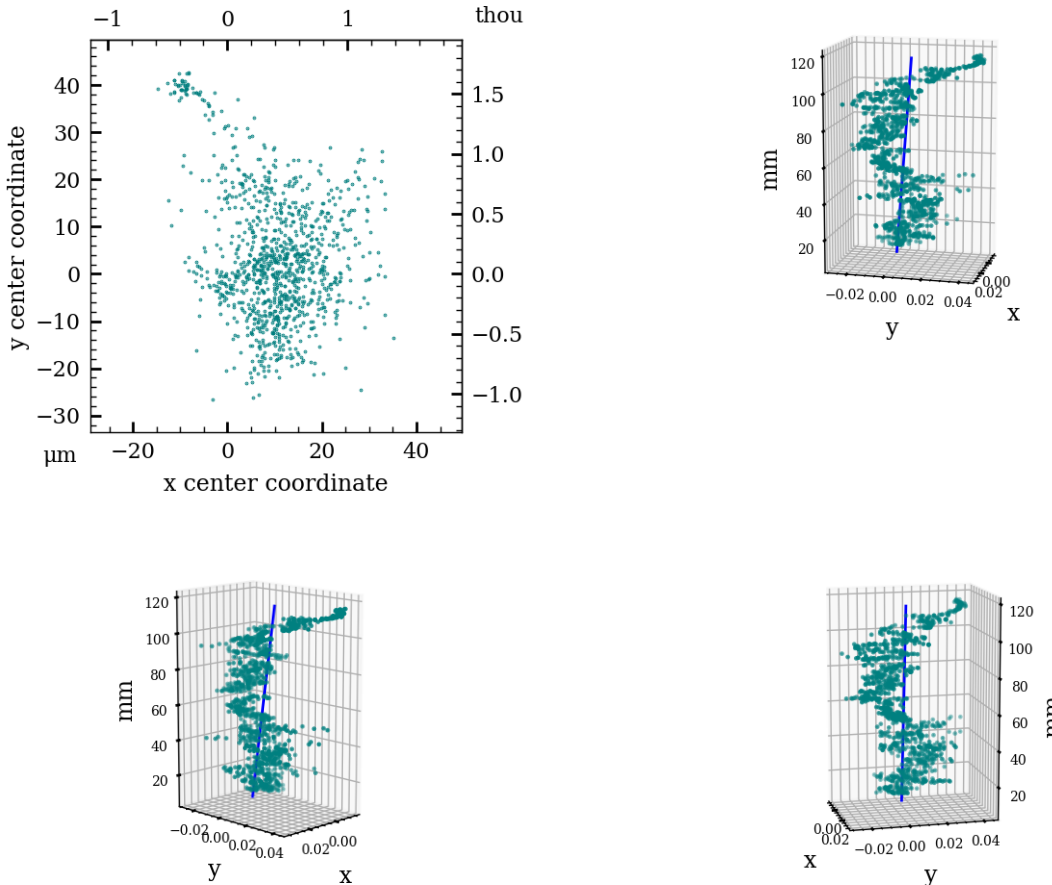


Figure 37: Coaxiality residual plots of exterior surface, PV001.

Coaxiality plots, interior surface



Coaxiality residuals from fitted axis, interior surface

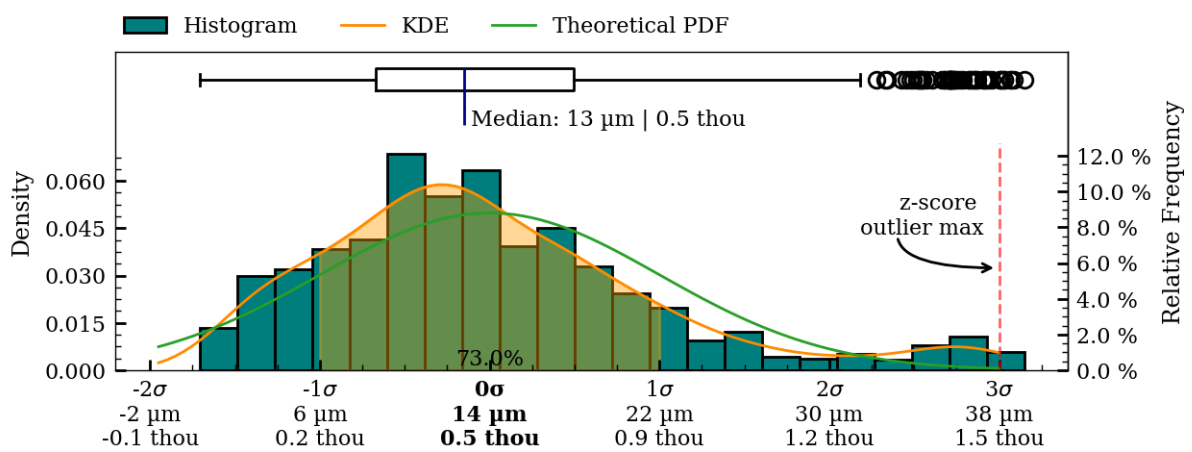


Figure 38: Coaxiality residual plots of interior surface, PV001.

Surface Variability

To illustrate the overall surface deviations of the object, a surface variability heatmap has been created. This heatmap provides an accessible overview of the topography of the manufacturing precision and surface structure of the object.

When CT scanning hard-stone objects, their internal crystalline structure will be captured by the scanner. This can result in strange-looking structures inside the walls of the scan. These structures have not all been filtered from the dataset, and can therefore be seen on the interior heatmap and will result in an increased total range of the surface deviation statistics.

The surface variability measurements are created by fitting a number of higher-order polynomials to the two-dimensional folded profile of the scan data. This process creates an idealized mathematical representation of actual surface curvature of object, and as such provides a continuous model representation of the actual object. It is important to note that only such a non-discretized representation is sufficient to avoid introducing inconsistently varying errors in the mapping of the final surface deviation results, that the rendered heatmaps are based on.

To produce the final surface variability map, the distance from each scanned vertex to the fitted polynomial is calculated and used as the mapping function input, for applying colours to the surface of the object.

It is important to note that this variability map does not describe deviations from the original *intended* shape of the artifact (if any), as this shape (the *intended design*, so to speak) will have been lost to time. It does however provide a very informative visualization of the texture and structure of the surface and very importantly, *does* highlight potential manufacturing-relevant patterns in the surface texture (if present). Such patterns are, as an example, clearly evident on the interior surface of artifact PV001.

Exterior surface

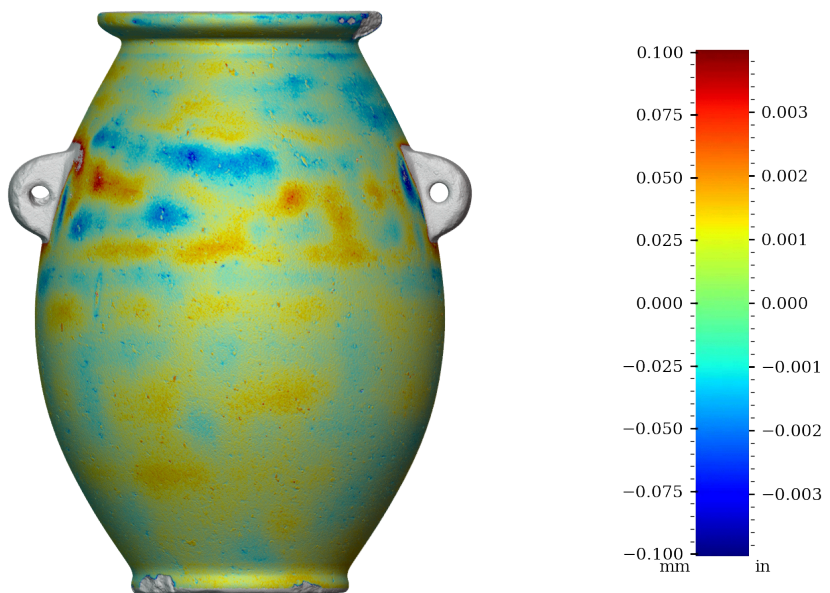


Figure 39: Surface variability heatmap of PV001, front view

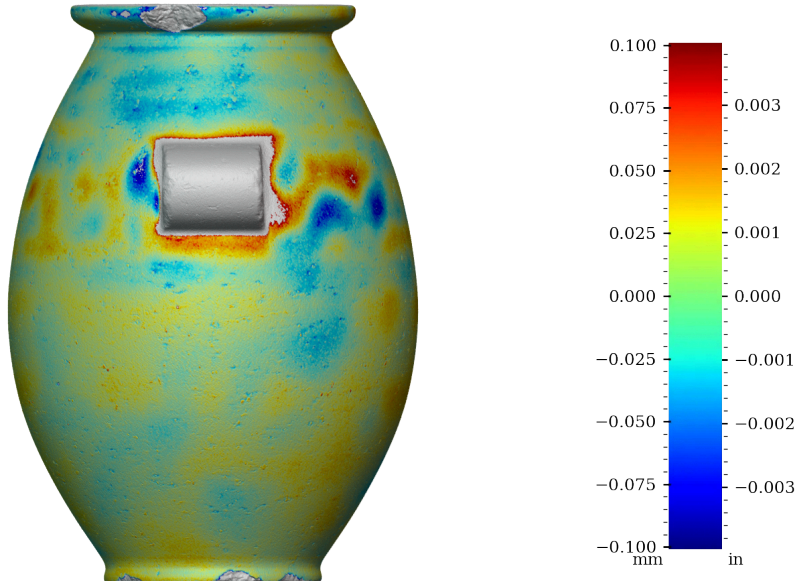


Figure 40: Surface variability heatmap of PV001, rotated 90°

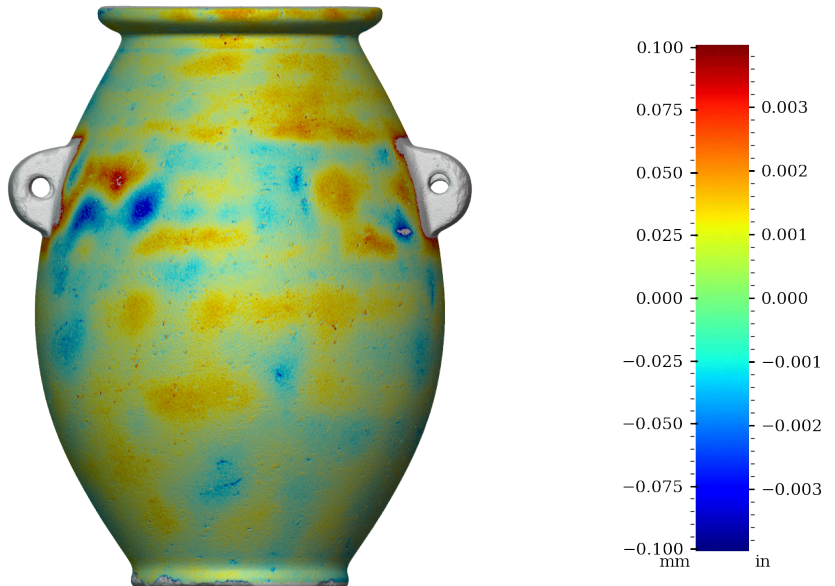


Figure 41: Surface variability heatmap of PV001, rotated 180°

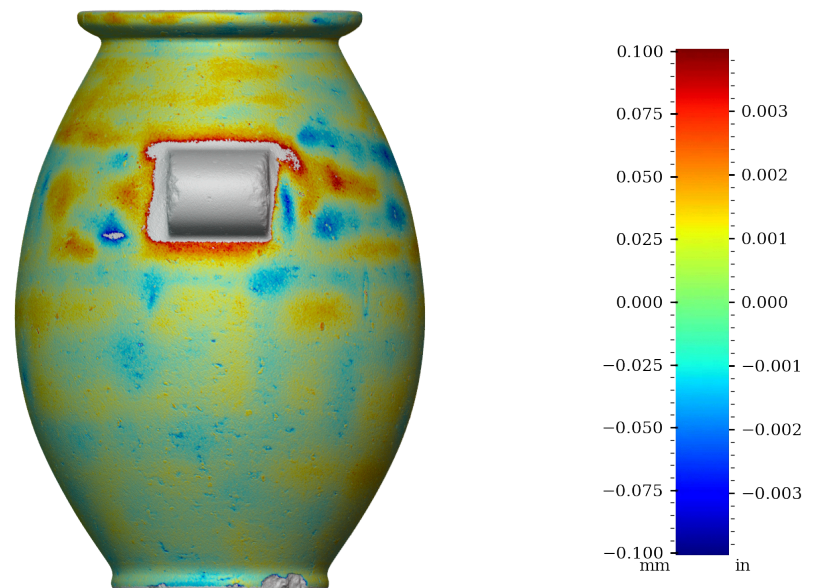


Figure 42: Surface variability heatmap of PV001, rotated 270°

Interior surface

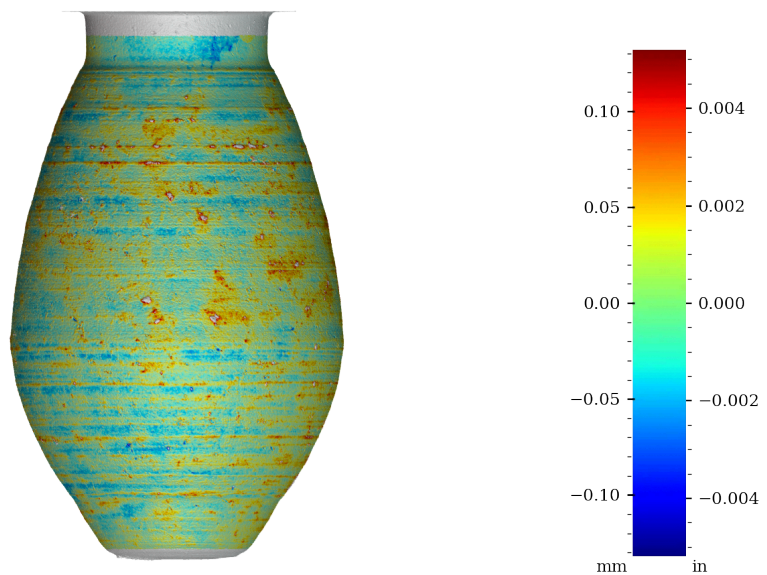


Figure 43: Surface variability heatmap of PV001, front view

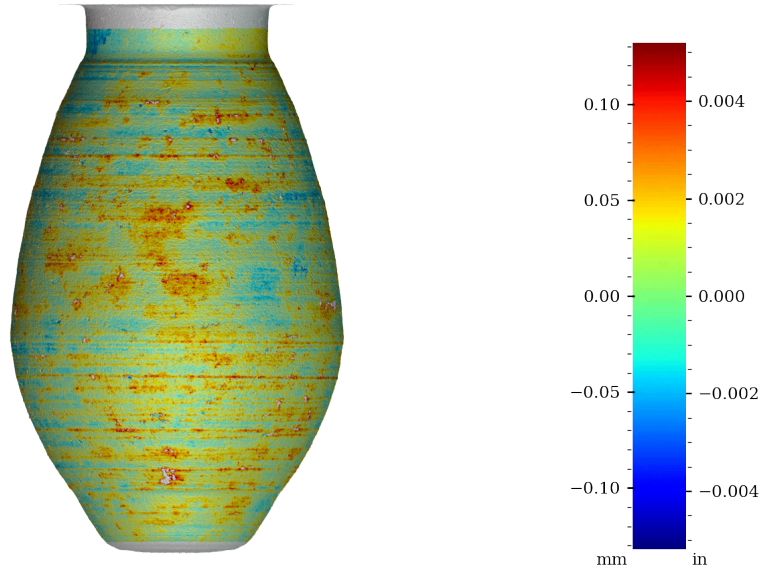


Figure 44: Surface variability heatmap of PV001, rotated 90°

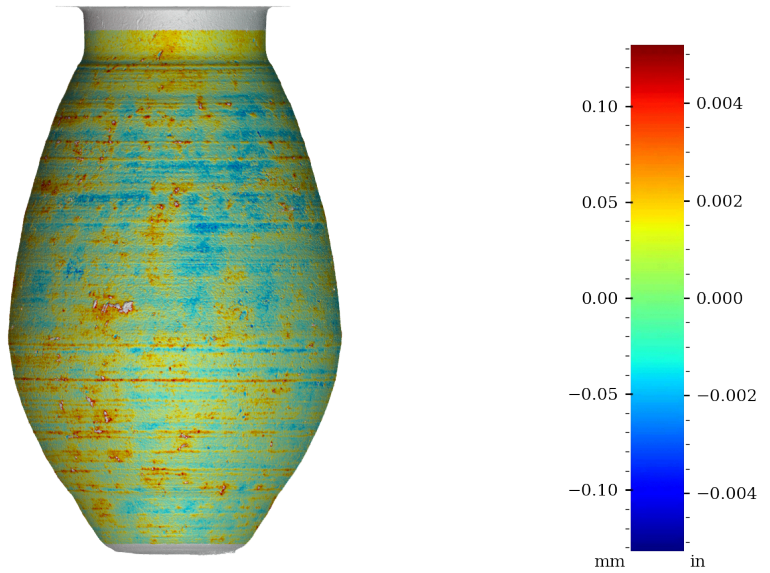


Figure 45: Surface variability heatmap of PV001, rotated 180°

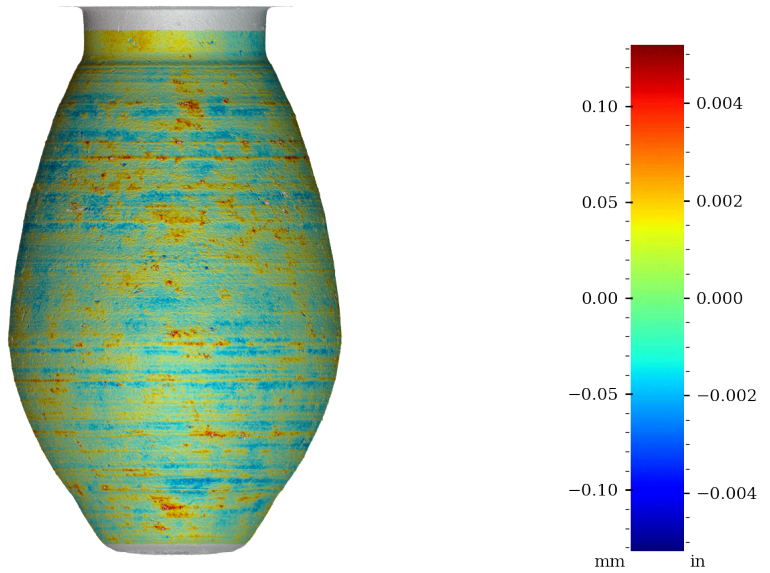


Figure 46: Surface variability heatmap of PV001, rotated 270°

Surface variability statistics

Area	MSD	RMSD	SD	Mean AD	Median AD	Range	Min	Max	Sample size
	mm ²	mm	mm	mm	mm	mm	mm	mm	
Exterior	0.0005	0.023	0.023	0.014	0.017	0.435	-0.218	0.217	931467
Interior	0.0014	0.038	0.038	0.023	0.028	1.023	-0.320	0.704	1158520
	in ²	in	in	in	in	in	in	in	
Exterior	0.000001	0.0009	0.0009	0.0005	0.0007	0.0171	-0.0086	0.0086	931467
Interior	0.000002	0.0015	0.0015	0.0009	0.0011	0.0403	-0.0126	0.0277	1158520

Table 5: Surface variability statistics, PV001

Table 5 shows the statistics of the distance from the scan vertices to the best fit object model. These statistics are briefly explained below.

Mean Squared Deviation (MSD), also known as Mean Squared Error (MSE).

$$\text{MSD} = \frac{\sum_{i=1}^n (y_i - \hat{y})^2}{n}$$

The MSD metric shows the average squared difference between the scanned points and the fitted composite polynomial model (a value of 0 would be a perfect match). This metric emphasizes imperfections in the surface of the artifact. Outliers will negatively influence this metric, raising the value of the MSE. This CT scan contains outliers in the form of scan points from the internal crystalline structures in the walls of the object. Not all of these outliers have been removed, which will raise the MSE metric (lowering the precision score).

Root Mean Squared Deviation (RMSD), also known as Root Mean Squared Error (RMSE).

$$\text{RMSD} = \sqrt{\frac{\sum_{i=1}^n (y_i - \hat{y})^2}{n}}$$

Measures the dispersion of the measured surface variability y_i around a model predictor (\hat{y}). By obtaining the root of the MSD, the exponent will be removed from the measurement, enabling comparisons with other statistics of the same unit and making it more accessible to those familiar with the RMSD metric. This measure is used to assess the fit of a regression model to a dataset, in this case our best fit composite polynomial model. The lower the RMSD metric, the better the fit.

Standard Deviation (SD)

$$s = \sqrt{\frac{\sum_{i=1}^n (y_i - \bar{y})^2}{n-1}}$$

Measures the dispersion of the measured surface variability y_i around the mean (\bar{y}). If the residuals are normally distributed around the mean ($\bar{y} \approx 0$), the SD will be equal to the RMSD. See Figure 47 and Figure 48

Mean Absolute Deviation (MeanAD)

$$\text{MeanAD} = \frac{\sum_{i=1}^n |y_i - \bar{y}|}{n}$$

This metric is similar to the SD, but the difference between the residuals and the mean is *not* squared. Instead of indicating the spread of the data, we look at the average distance between each data point and the mean. The Mean Absolute Deviation is affected less by outliers than the Standard Deviation.

Median Absolute Deviation (MedianAD)

$$\text{MedianAD} = \text{median}(|y_i - \text{median}(y)|)$$

The Median Absolute Deviation is a measure of the dispersion of the data around the median.

Range

$$\max(y_i) - \min(y_i)$$

Range is a measure of the total spread of the residuals

Histogram, KDE and Box-plot of measured surface variability - exterior surface

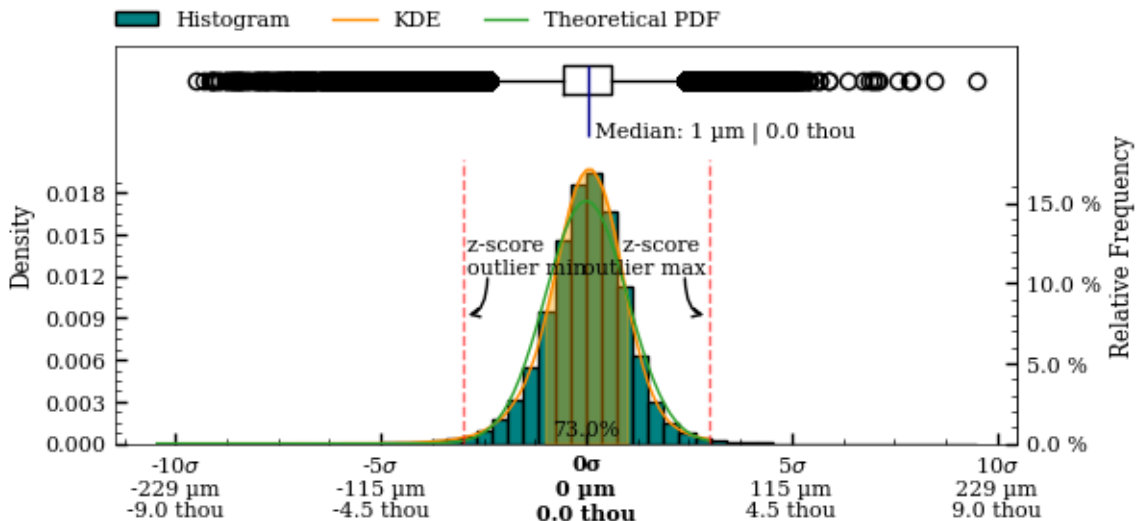


Figure 47: Exterior surface variability boxplot, kds and histogram.

Histogram, KDE and Box-plot of measured surface variability - interior surface

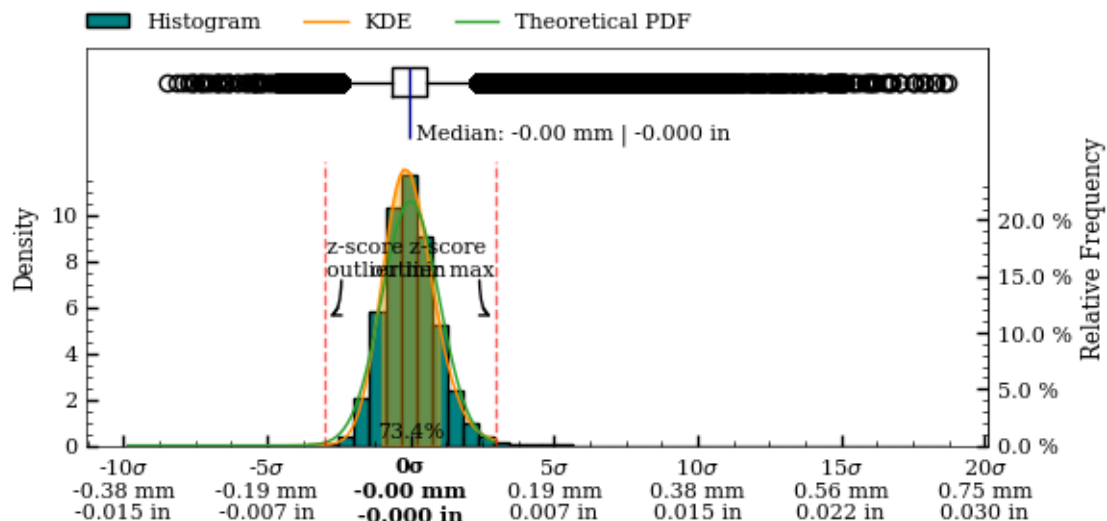


Figure 48: Interior surface variability boxplot, kds and histogram.

Precision Score Of The Artifact

To enable valid comparison of the manufacturing precision of different artifacts, a metric that robustly quantifies the overall precision of the object is required. The considerations for such a metric will be explored in this section.

Based on these considerations, a *Precision Score* metric will be defined.

For an object to be described as having been manufactured with high precision, several qualities must be present *concurrently*, and throughout the *entire* geometry of the final object. A given object may exhibit high levels of one or more *components* of precision, but be lacking in others. For example:

- An object may present high levels of coaxiality, but lack circularity.
- An object may exhibit good circularity, but show imperfections in the surface structure.
- An object may be smoothed to perfection *without* any circularity or coaxiality.
- An object may exhibit high levels of all of the above metrics in *some* areas, but not in others.

Therefore, a precision score metric **must** account for *all* aspects of the individual, underlying precision metrics (circularity, concentricity, coaxiality and surface variability) throughout the *entire* surface area of the object.

The composite high order polynomial model, used to generate the surface variability map (described in Surface Variability, p. 41) is the best continuous mathematical representation of the object available to us (lacking any original design plans, as would normally be available in metrological analysis). This idealized model encompasses all of the above component metrics.

In the creation of the model, all scan data-points are taken into account (excluding areas with extensive damage), making it the best possible idealized representation we can achieve. When this model has been accurately created, the deviation between the model and the scanned data-points can be calculated over the non-discretized polynomials, *without* the need for an “original” CAD model (and importantly, unless such a CAD model *actually* corresponded to the original design intent, it would be an insufficient comparison basis).

Within the context of defining a valid, overall precision metric, this approach satisfies the incorporation of all of the necessary metrics:

- **Circularity:** Because the reconstructed polynomial model is revolved around the Z-plane, the idealized representation is perfectly circular, and thus incorporates the circularity component.
- **Concentricity and coaxiality:** Because the Z-axis (datum axis) is the center axis of the model, it incorporates the concentricity and coaxiality components.
- **Surface variability:** Because the model is continuous and non-discretized, it can be used accurately for all points of the scan data, and incorporates the surface variability component.

The level of precision ultimately achieved in a physical object does not share a linear relationship with its manufacturing requirements. Since continuously higher levels of final precision becomes progressively harder to achieve, an overall precision metric must take this relationship into account.

A robust statistical metric that satisfies this requirement is the *Mean Squared Deviation* (MSD or MSE). Here specifically, we can utilize the mean square of the deviations between the model (\hat{y}) and the data-points (y_i).

Combining all of the above considerations, we can express a well-defined *Precision Score* metric, that provides an immediately accessible way to understand the overall precision of an object, while being statistically valid. Since the Mean Squared Deviation tends towards zero as the overall precision increases, the inverse of the Mean Squared Deviation is taken to obtain a precision score metric that increases as precision increases¹³:

$$\text{Precision Score} = \frac{n}{\sum_{i=1}^n (y_i - \hat{y})^2}$$

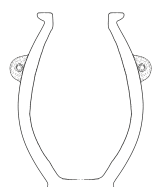
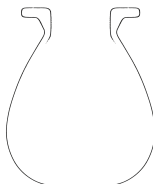
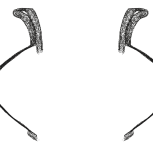
¹³The precision score unit is $\frac{1}{\text{mm}^2}$

A precision score will be calculated separately for:

- The exterior surface
- The interior surface
- The full surface

As most scans do not include sufficient scan data for the interior surface, the exterior surface will be used for calculating the precision score in most cases. In the rare case that the scan data is more complete for the *interior* surface, this will be used instead.

Table 6 shows the precision score of this artifact (PV001), compared to the two most precise, and the two least precise vessels currently analyzed.

Artifact		Material	Precision Score	Link to Report
		PV001 Red Granite	1905 Full: 980 Exterior: 1905 Interior: 705	Report Publication
		PV006 Dark grey granite	621 Full: 521 Exterior: 621 Interior: 152	Report Publication
		MV001 Pottery	1.93 Full: 1.92 Exterior: 1.93 Interior: 1.85	Report Publication (Draft - Awaiting publication)
		MV010 Calcite (Egyptian Alabaster)	1.12 Full: 0.64 Exterior: 1.12 Interior: 0.20	Report Publication (Draft - Awaiting publication)

Analysis Roadmap

While the current iteration of this work already provides valuable results, continued future additions and improvements will enhance their utility further. This section details planned iterative updates and improvements, to both the reports themselves, and to the underlying methodology and software they are created with.

Alignment Section

- Detailed exploration of different circle regression algorithms
- If handles are present on the vessel, exploring alignment of the vessels so the handle positions match each other
- Add optimization of the perpendicular surface deviation, with the best results of the coaxial alignment
- Align by minimizing circularity results (of rotated sample slice, to compensate for sample height distortions)

Measurements of Precision

- Section detailing how measurements perpendicular to the surface curvature are obtained
- Detailed surface area analysis, exploring the residual patterns throughout subsequent sample slices of the artifact surface
- Wall thickness deviation color map
- Robust outlier identification on circularity, to better handle analysis of damaged areas of the artifacts in addition to removal of interior crystalline structure points present in CT scans
- Layout updates to the charts and tables

Visibility of Outliers and Damaged Sections

- Identification and marking of damaged parts
- Visualization of outliers on the artifact surface

Exploration of Mathematical Primitives

- Analysis of selected curvatures and flat surfaces on the vessel in both the horizontal and vertical planes
 - Circles
 - Parabolas
 - Ellipsoids
 - Hyperbolas
 - Cones
- Implementation of robust regressions models suitable for this domain, based on RANSAC.

Metrics on Primary Features

- Measurements of features in the horizontal plane
- Measurements of features in the vertical plane
- Measurements of angles
- Measurements of volume

Exploration of Potential Design Ratios

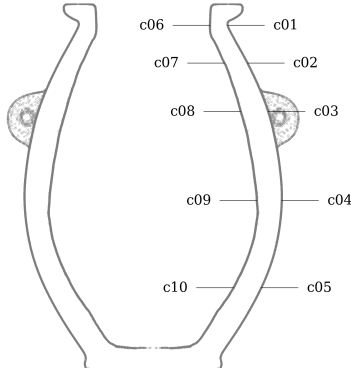
- $\pi, \varphi, e, 1, 2, 3, 4$ etc.

Raw Dataset Attachments

- Including all measurement and sample coordinates as CSV-files embedded in the report
- Including an STL file of the aligned object alongside the report, for easier external replication and validation of the research results

Appendix A - Comparison Of Circularity Measurements (Z-plane vs. surface-perpendicular)

Comparison of circularity samples



Samples perpendicular to the surface curvature

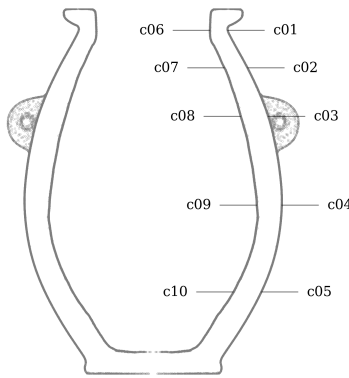
Tag	Area	Measured deviation ⁹	Residuals				Sample size	Slice		
			Range	RMSD ¹⁰	MAD ¹¹	SD		Height	Z coord.	Radius ¹²
		mm	mm	mm	mm	mm	mm	mm	mm	mm
c01	exterior	$\bar{\Omega}49.103 \pm 0.069$	0.114	0.019	0.012	0.019	473	0.100	113.516	24.551
c02	exterior	$\bar{\Omega}62.221 \pm 0.075$	0.128	0.025	0.019	0.025	585	0.100	101.108	31.110
c03	exterior	$\bar{\Omega}75.848 \pm 0.101$	0.197	0.036	0.024	0.035	612	0.100	85.163	37.924
c04	exterior	$\bar{\Omega}84.772 \pm 0.081$	0.141	0.019	0.013	0.017	921	0.100	55.890	42.386
c05	exterior	$\bar{\Omega}71.251 \pm 0.065$	0.114	0.017	0.012	0.017	711	0.100	27.256	35.626
c06	interior	$\bar{\Omega}37.457 \pm 0.120$	0.194	0.037	0.029	0.037	531	0.100	113.516	18.728
c07	interior	$\bar{\Omega}47.060 \pm 0.163$	0.255	0.033	0.021	0.033	676	0.100	101.108	23.530
c08	interior	$\bar{\Omega}57.791 \pm 0.222$	0.319	0.036	0.023	0.035	1119	0.100	85.163	28.896
c09	interior	$\bar{\Omega}68.374 \pm 0.142$	0.238	0.031	0.021	0.031	1305	0.100	55.890	34.187
c10	interior	$\bar{\Omega}52.949 \pm 0.118$	0.230	0.033	0.023	0.033	878	0.100	27.256	26.475

Table 7: Detailed circularity measurements at selected samples in z-plane, vessel PV001.

Samples in the Z-plane

Tag	Area	Measured deviation ⁹	Residuals				Sample size	Slice		
			Range	RMSD ¹⁰	MAD ¹¹	SD		Height	Z coord.	Radius ¹²
		mm	mm	mm	mm	mm	mm	mm	mm	mm
c01	exterior	$\bar{\Omega}49.102 \pm 0.059$	0.112	0.020	0.013	0.020	503	0.100	113.516	24.551
c02	exterior	$\bar{\Omega}62.227 \pm 0.103$	0.190	0.031	0.022	0.031	735	0.100	101.108	31.114
c03	exterior	$\bar{\Omega}75.871 \pm 0.127$	0.235	0.039	0.026	0.039	691	0.100	85.163	37.936
c04	exterior	$\bar{\Omega}84.789 \pm 0.090$	0.141	0.017	0.010	0.017	922	0.100	55.890	42.394
c05	exterior	$\bar{\Omega}71.257 \pm 0.089$	0.159	0.024	0.017	0.024	882	0.100	27.256	35.629
c06	interior	$\bar{\Omega}37.477 \pm 0.130$	0.194	0.037	0.027	0.037	535	0.100	113.516	18.738
c07	interior	$\bar{\Omega}47.055 \pm 0.144$	0.246	0.037	0.025	0.037	837	0.100	101.108	23.528
c08	interior	$\bar{\Omega}57.809 \pm 0.214$	0.353	0.038	0.024	0.038	1232	0.100	85.163	28.905
c09	interior	$\bar{\Omega}68.366 \pm 0.144$	0.238	0.032	0.020	0.032	1309	0.100	55.890	34.183
c10	interior	$\bar{\Omega}52.955 \pm 0.150$	0.269	0.042	0.027	0.041	1129	0.100	27.256	26.478

Table 8: Detailed circularity measurements at selected samples perpendicular to vessel curvature, vessel PV001.



Samples perpendicular to the surface curvature

Tag	Area	Measured deviation ⁹	Residuals				Sample size	Slice		
			Range	RMSD ¹⁰	MAD ¹¹	SD		Height	Z coord.	Radius ¹²
			in	in	in	in		in	in	in
c01	exterior	$\varnothing 1.9332 \pm 0.0027$	0.0045	0.0007	0.0005	0.0007	473	0.0039	4.4691	0.9666
c02	exterior	$\varnothing 2.4496 \pm 0.0029$	0.0050	0.0010	0.0007	0.0010	585	0.0039	3.9806	1.2248
c03	exterior	$\varnothing 2.9861 \pm 0.0040$	0.0078	0.0014	0.0010	0.0014	612	0.0039	3.3529	1.4931
c04	exterior	$\varnothing 3.3375 \pm 0.0032$	0.0056	0.0007	0.0005	0.0007	921	0.0039	2.2004	1.6687
c05	exterior	$\varnothing 2.8052 \pm 0.0026$	0.0045	0.0007	0.0005	0.0007	711	0.0039	1.0731	1.4026
c06	interior	$\varnothing 1.4747 \pm 0.0047$	0.0076	0.0015	0.0011	0.0014	531	0.0039	4.4691	0.7373
c07	interior	$\varnothing 1.8528 \pm 0.0064$	0.0100	0.0013	0.0008	0.0013	676	0.0039	3.9806	0.9264
c08	interior	$\varnothing 2.2753 \pm 0.0087$	0.0126	0.0014	0.0009	0.0014	1119	0.0039	3.3529	1.1376
c09	interior	$\varnothing 2.6919 \pm 0.0056$	0.0094	0.0012	0.0008	0.0012	1305	0.0039	2.2004	1.3459
c10	interior	$\varnothing 2.0846 \pm 0.0046$	0.0090	0.0013	0.0009	0.0013	878	0.0039	1.0731	1.0423

Table 9: Detailed circularity measurements at selected samples in z-plane, vessel PV001.

Samples in the Z-plane

Tag	Area	Measured deviation ⁹	Residuals				Sample size	Slice		
			Range	RMSD ¹⁰	MAD ¹¹	SD		Height	Z coord.	Radius ¹²
			in	in	in	in		in	in	in
c01	exterior	$\varnothing 1.9331 \pm 0.0023$	0.0044	0.0008	0.0005	0.0008	503	0.0039	4.4691	0.9666
c02	exterior	$\varnothing 2.4499 \pm 0.0040$	0.0075	0.0012	0.0009	0.0012	735	0.0039	3.9806	1.2249
c03	exterior	$\varnothing 2.9871 \pm 0.0050$	0.0093	0.0015	0.0010	0.0015	691	0.0039	3.3529	1.4935
c04	exterior	$\varnothing 3.3381 \pm 0.0035$	0.0055	0.0007	0.0004	0.0007	922	0.0039	2.2004	1.6691
c05	exterior	$\varnothing 2.8054 \pm 0.0035$	0.0063	0.0009	0.0007	0.0009	882	0.0039	1.0731	1.4027
c06	interior	$\varnothing 1.4755 \pm 0.0051$	0.0077	0.0015	0.0010	0.0014	535	0.0039	4.4691	0.7377
c07	interior	$\varnothing 1.8526 \pm 0.0057$	0.0097	0.0015	0.0010	0.0015	837	0.0039	3.9806	0.9263
c08	interior	$\varnothing 2.2760 \pm 0.0084$	0.0139	0.0015	0.0009	0.0015	1232	0.0039	3.3529	1.1380
c09	interior	$\varnothing 2.6916 \pm 0.0057$	0.0094	0.0013	0.0008	0.0012	1309	0.0039	2.2004	1.3458
c10	interior	$\varnothing 2.0849 \pm 0.0059$	0.0106	0.0016	0.0011	0.0016	1129	0.0039	1.0731	1.0424

Table 10: Detailed circularity measurements at selected samples perpendicular to vessel curvature, vessel PV001.

Comparison of circularity on the full vessel surface

Metric

Samples perpendicular to the surface curvature

Area	Range			Standard Deviation			Median Absolute Deviation			Slices	Slice height
	Median	Min.	Max.	Median	Min.	Max.	Median	Min.	Max.		
	mm	mm	mm	mm	mm	mm	mm	mm	mm		
Exterior	0.126	0.072	0.307	0.018	0.012	0.042	0.002	0.007	0.025	1190	0.100
Interior	0.235	0.103	0.800	0.033	0.019	0.081	0.002	0.011	0.036	1065	0.100

Table 11: Detailed circularity measurements at selected samples in z-plane, vessel PV001.

Samples in the z-plane

Area	Range			Standard Deviation			Median Absolute Deviation			Slices	Slice height
	Median	Min.	Max.	Median	Min.	Max.	Median	Min.	Max.		
	mm	mm	mm	mm	mm	mm	mm	mm	mm		
Exterior	0.157	0.090	0.457	0.025	0.015	0.084	0.004	0.009	0.064	1187	0.100
Interior	0.260	0.160	0.829	0.036	0.026	0.081	0.002	0.016	0.047	1060	0.100

Table 12: Detailed circularity measurements at selected samples perpendicular to vessel curvature, vessel PV001.

Imperial

Samples perpendicular to the surface curvature

Area	Range			Standard Deviation			Median Absolute Deviation			Slices	Slice height
	Median	Min.	Max.	Median	Min.	Max.	Median	Min.	Max.		
	in	in	in	in	in	in	in	in	in		
Exterior	0.126	0.072	0.307	0.018	0.012	0.042	0.002	0.007	0.025	1190	0.100
Interior	0.235	0.103	0.800	0.033	0.019	0.081	0.002	0.011	0.036	1065	0.100

Table 13: Detailed circularity measurements at selected samples in z-plane, vessel PV001.

Samples in the z-plane

Area	Range			Standard Deviation			Median Absolute Deviation			Slices	Slice height
	Median	Min.	Max.	Median	Min.	Max.	Median	Min.	Max.		
	in	in	in	in	in	in	in	in	in		
Exterior	0.157	0.090	0.457	0.025	0.015	0.084	0.004	0.009	0.064	1187	0.100
Interior	0.260	0.160	0.829	0.036	0.026	0.081	0.002	0.016	0.047	1060	0.100

Table 14: Detailed circularity measurements at selected samples perpendicular to vessel curvature, vessel PV001.

Circularity analysis of exterior samples perpendicular to surface curvature

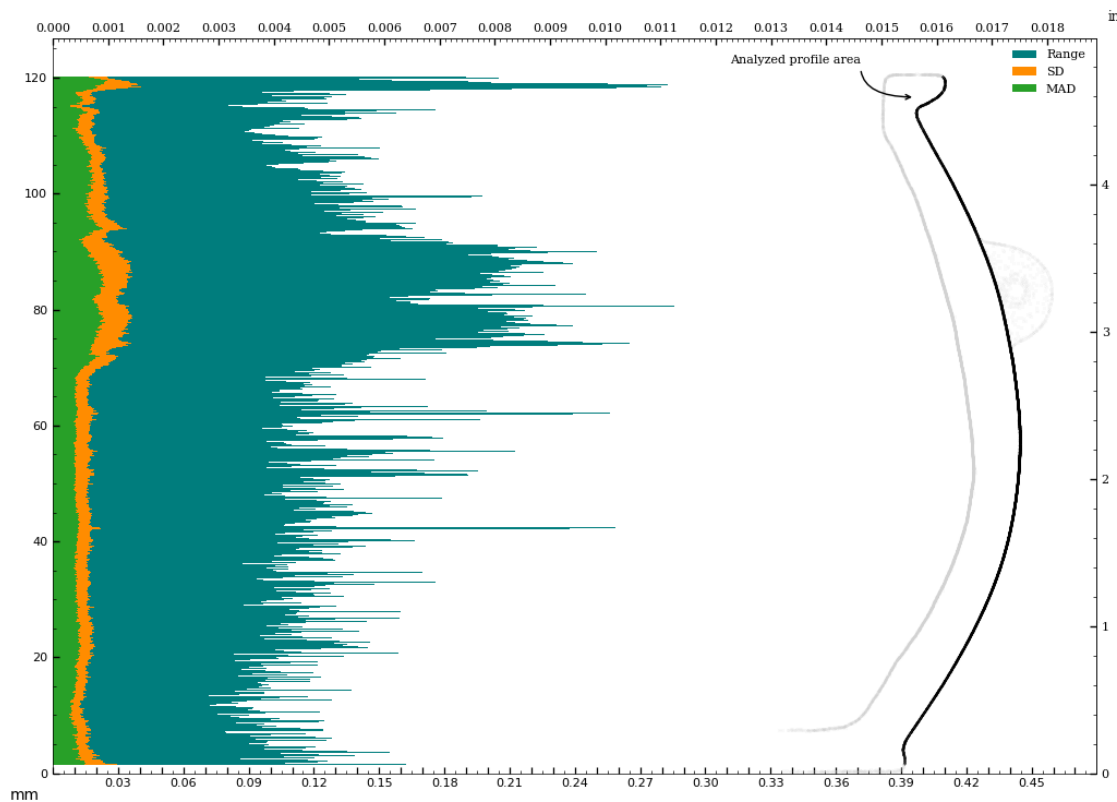


Figure 49: Circularity analysis of exterior samples perpendicular to surface curvature

Circularity analysis of exterior surface - in z-plane

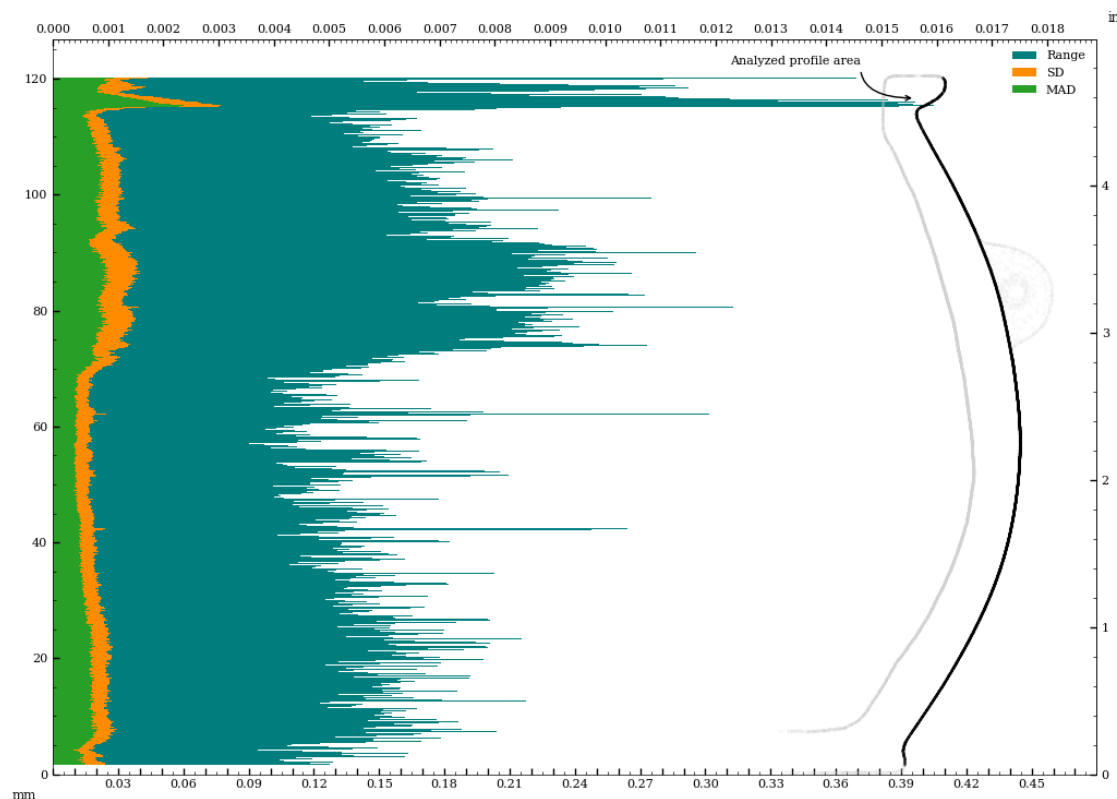


Figure 50: Circularity analysis of exterior surface - in z-plane

Circularity analysis of exterior samples perpendicular to surface curvature

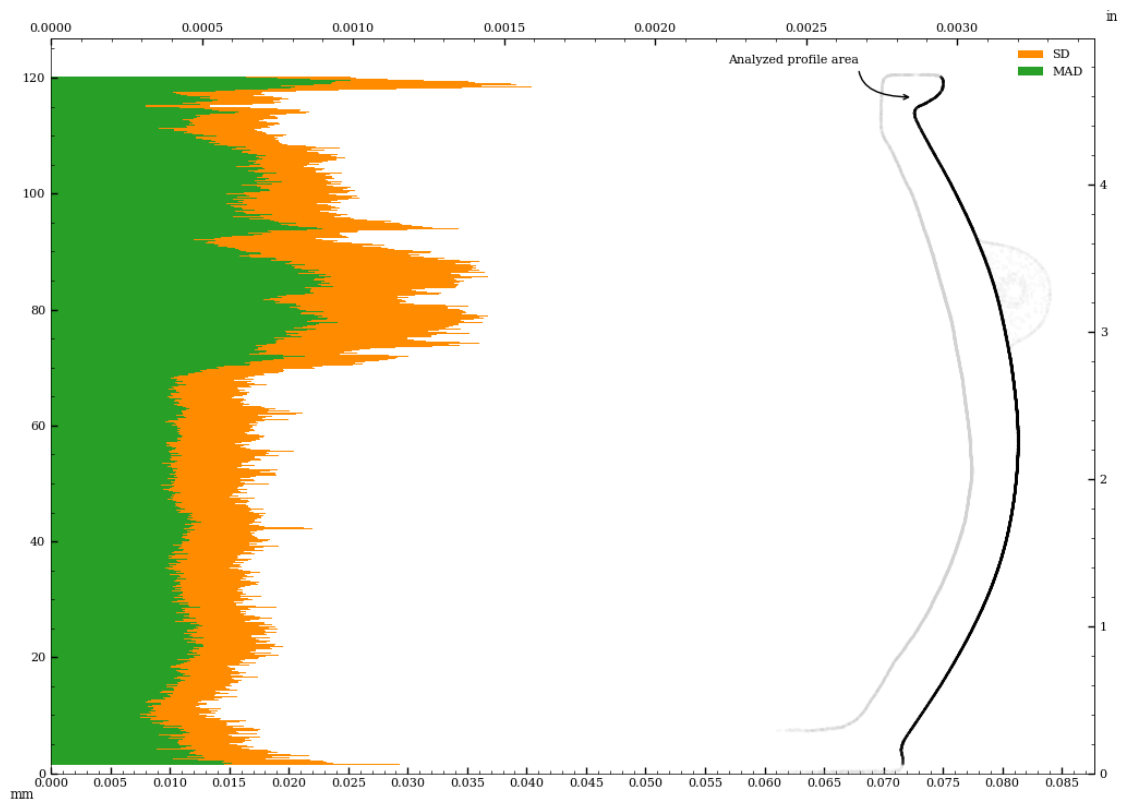


Figure 51: Circularity analysis of exterior samples perpendicular to surface curvature

Circularity analysis of exterior surface - in z-plane

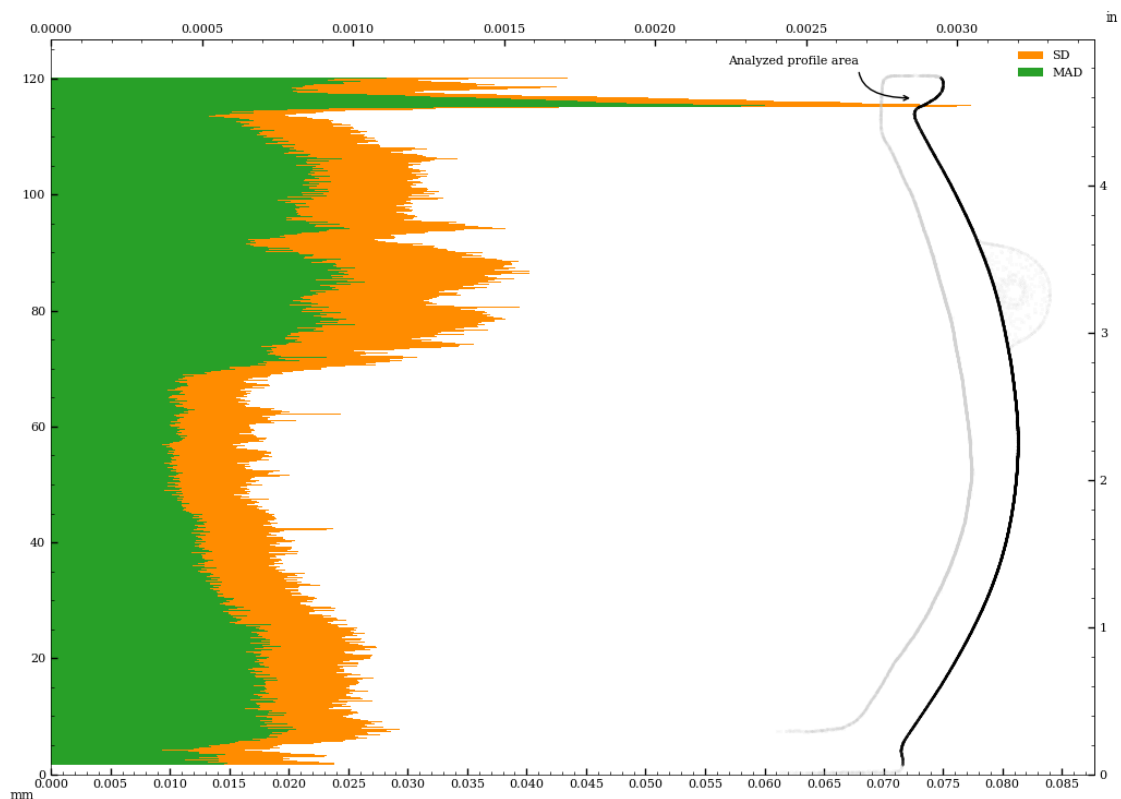


Figure 52: Circularity analysis of exterior surface - in z-plane

Circularity analysis of interior samples perpendicular to surface curvature

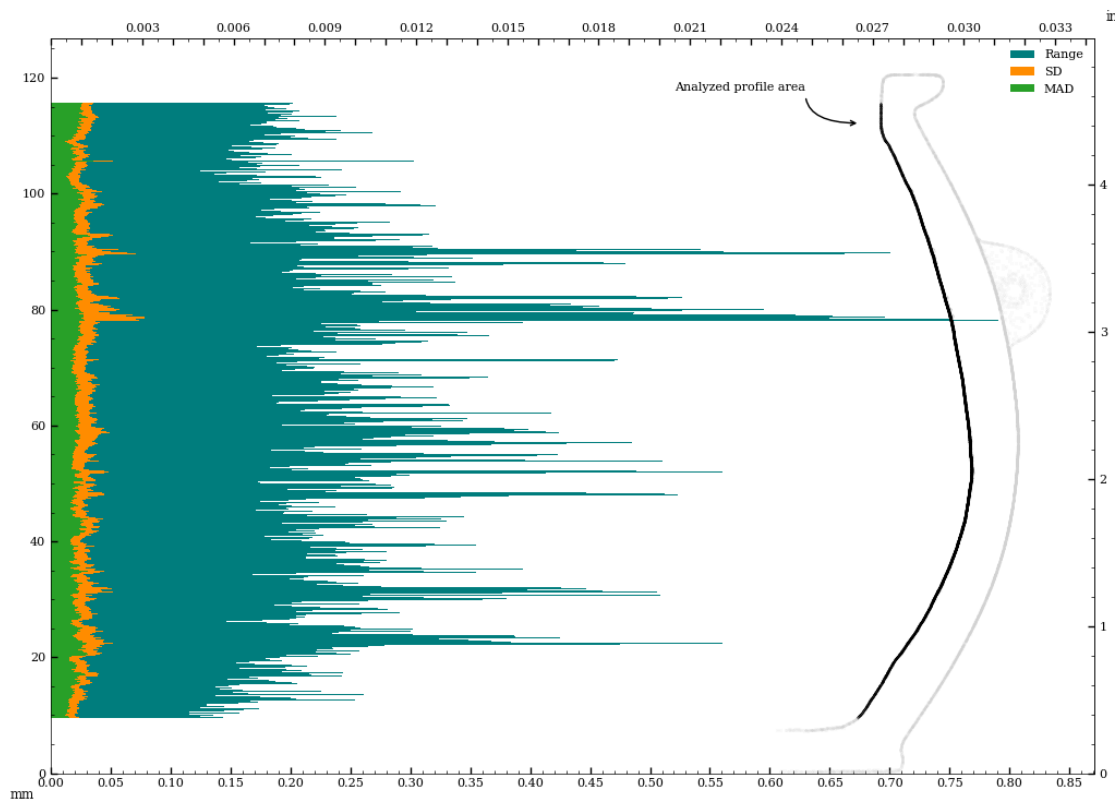


Figure 53: Circularity analysis of interior samples perpendicular to surface curvature

Circularity analysis of interior surface - in z-plane

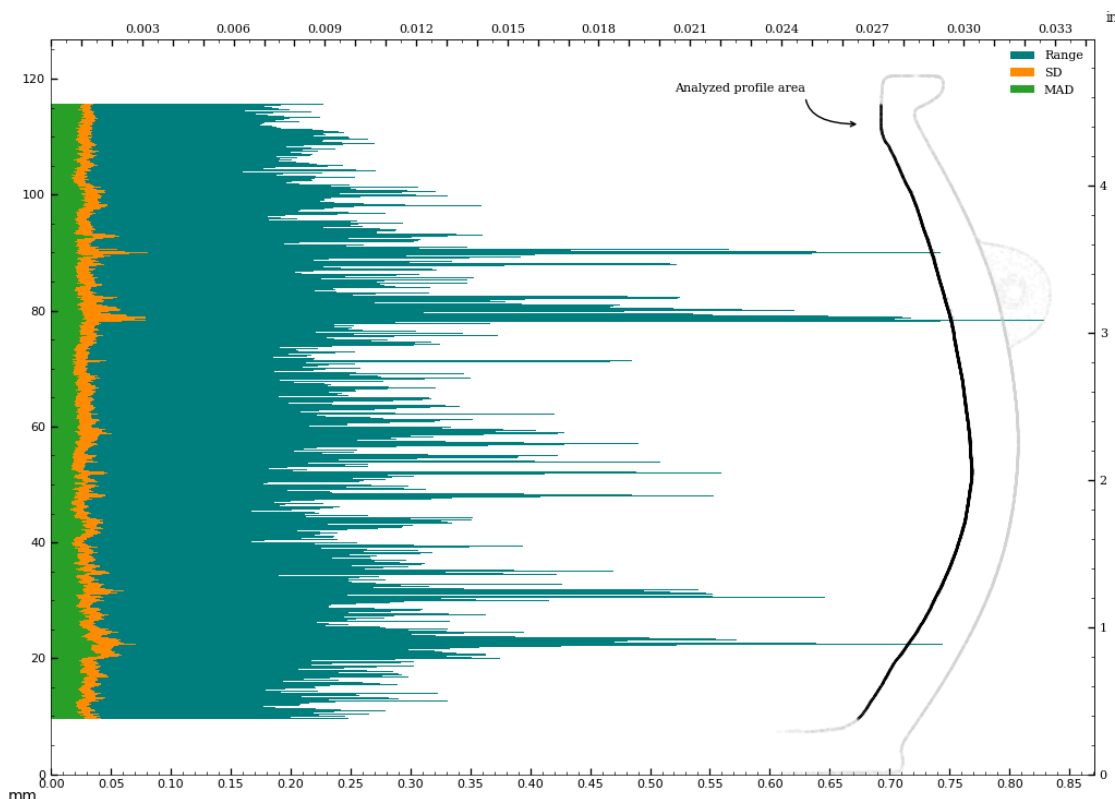


Figure 54: Circularity analysis of interior surface - in z-plane

Circularity analysis of interior samples perpendicular to surface curvature

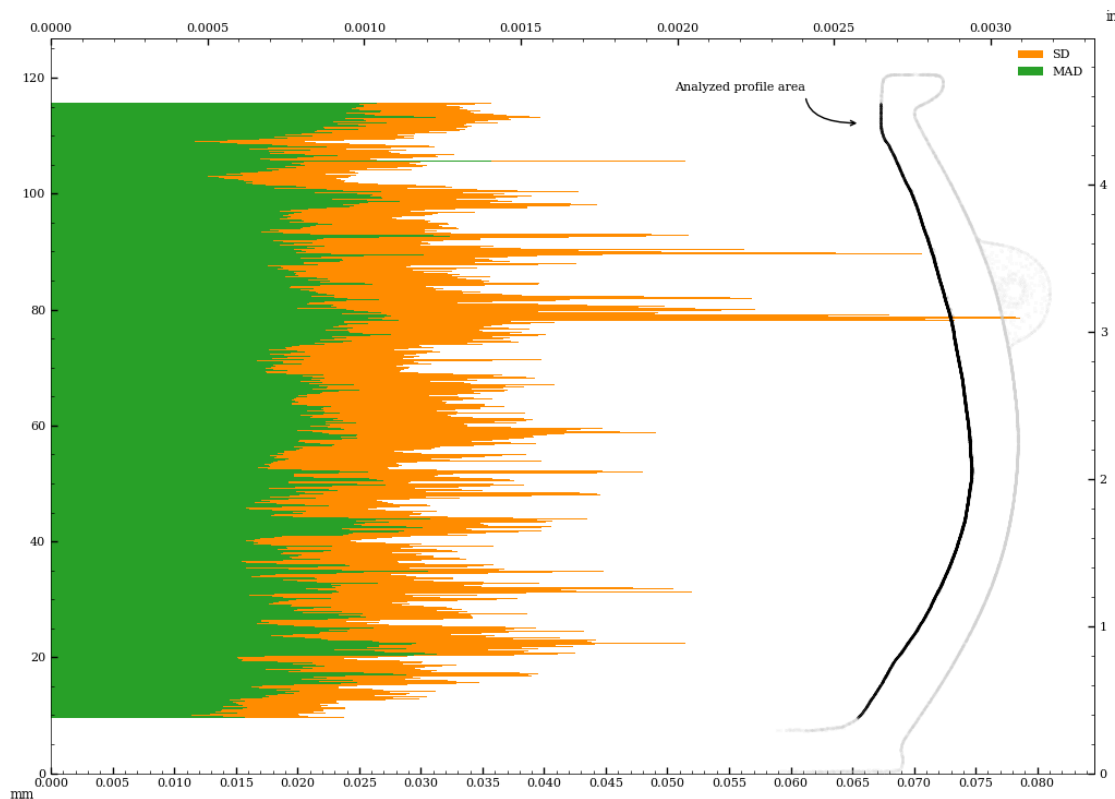


Figure 55: Circularity analysis of interior samples perpendicular to surface curvature

Circularity analysis of interior surface - in z-plane

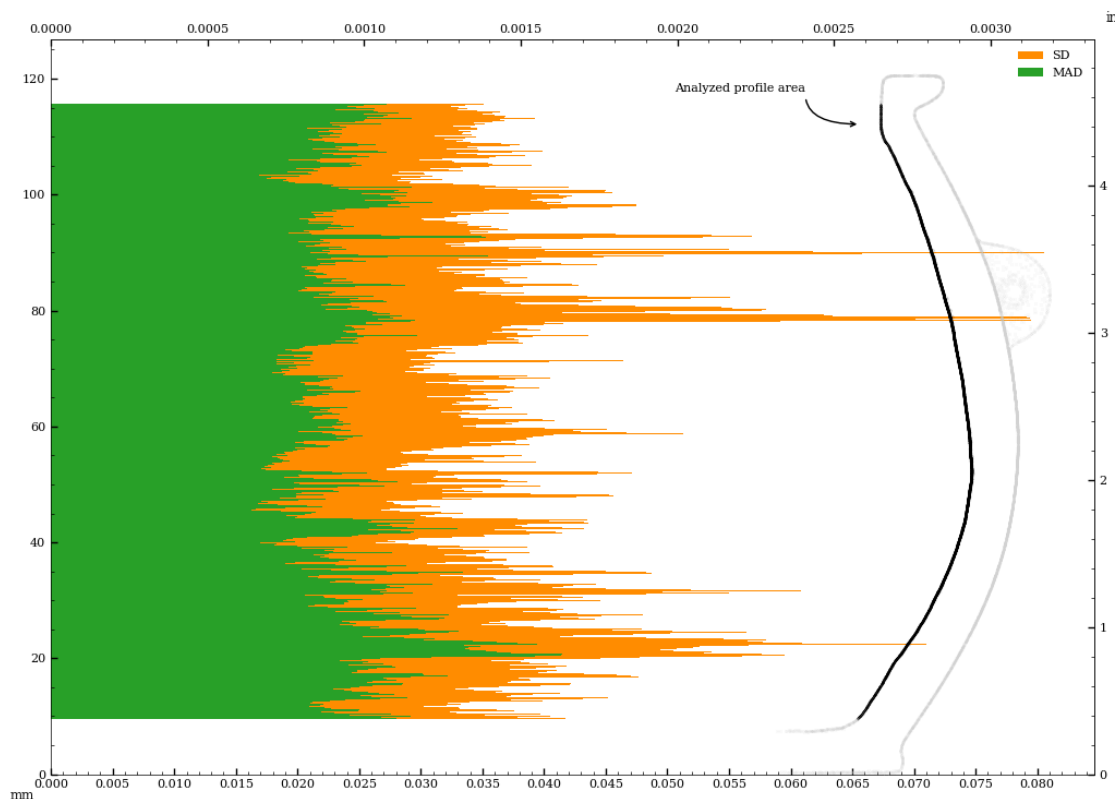


Figure 56: Circularity analysis of interior surface - in z-plane

Appendix B - Comparison Of Concentricity Measurements (Z-plane vs. surface-perpendicular)

Metric

Concentricity measurements perpendicular to surface curvature

Tag	Reference	Deviation	Sample size	Circle fit residuals analysis for sample listed in Tag column						
				Range full	Range inliers	SD full	SD inliers	MAD full	MAD inliers	Center (x,y)
			mm	mm	mm	mm	mm	mm	mm	μm
c01	z-axis	0.011	473	0.114	0.085	0.019	0.018	0.012	0.012	-6, 9
c02	z-axis	0.023	585	0.128	0.128	0.025	0.024	0.019	0.018	-19, 13
c03	z-axis	0.012	612	0.197	0.186	0.035	0.033	0.023	0.023	-12, 2
c04	z-axis	0.004	921	0.141	0.078	0.017	0.015	0.010	0.010	-2, 3
c05	z-axis	0.005	711	0.114	0.095	0.017	0.016	0.011	0.011	3, -4
c06	z-axis	0.042	531	0.194	0.159	0.037	0.035	0.027	0.025	-12, 40
c07	z-axis	0.011	676	0.255	0.191	0.033	0.029	0.021	0.021	10, 4
c08	z-axis	0.023	1119	0.319	0.196	0.035	0.032	0.021	0.021	11, -20
c09	z-axis	0.019	1305	0.238	0.173	0.031	0.029	0.020	0.020	19, -1
c10	z-axis	0.028	878	0.230	0.185	0.033	0.031	0.023	0.023	27, -5
c01	c06	0.032	473	0.114	0.085	0.019	0.018	0.012	0.012	5, -32
c02	c07	0.030	585	0.128	0.128	0.025	0.024	0.019	0.018	-29, 9
c03	c08	0.032	612	0.197	0.186	0.035	0.033	0.023	0.023	-23, 22
c04	c09	0.021	921	0.141	0.078	0.017	0.015	0.010	0.010	-21, 4
c05	c10	0.025	711	0.114	0.095	0.017	0.016	0.011	0.011	-25, 0

Concentricity measurements in z-plane

Tag	Reference	Deviation	Sample size	Circle fit residuals analysis for sample listed in Tag column						
				Range full	Range inliers	SD full	SD inliers	MAD full	MAD inliers	Center (x,y)
			mm	mm	mm	mm	mm	mm	mm	μm
c01	z-axis	0.013	503	0.121	0.119	0.023	0.022	0.013	0.013	-8, 10
c02	z-axis	0.027	735	0.192	0.162	0.032	0.031	0.024	0.024	-23, 14
c03	z-axis	0.015	691	0.238	0.207	0.039	0.038	0.025	0.025	-15, 3
c04	z-axis	0.004	922	0.141	0.086	0.017	0.016	0.011	0.010	-2, 3
c05	z-axis	0.006	882	0.150	0.129	0.025	0.023	0.017	0.016	4, -5
c06	z-axis	0.042	535	0.266	0.246	0.063	0.062	0.054	0.051	-12, 40
c07	z-axis	0.015	837	0.254	0.208	0.039	0.037	0.028	0.027	14, 7
c08	z-axis	0.023	1232	0.360	0.218	0.045	0.042	0.029	0.028	11, -20
c09	z-axis	0.020	1309	0.238	0.170	0.031	0.028	0.020	0.019	19, -1
c10	z-axis	0.038	1129	0.261	0.206	0.040	0.037	0.027	0.026	38, -6
c01	c06	0.031	503	0.121	0.119	0.023	0.022	0.013	0.013	4, -31
c02	c07	0.038	735	0.192	0.162	0.032	0.031	0.024	0.024	-37, 8
c03	c08	0.035	691	0.238	0.207	0.039	0.038	0.025	0.025	-26, 23
c04	c09	0.022	922	0.141	0.086	0.017	0.016	0.011	0.010	-21, 5
c05	c10	0.034	882	0.150	0.129	0.025	0.023	0.017	0.016	-34, 0

Imperial

Concentricity measurements perpendicular to surface curvature

Tag	Reference	Deviation	Sample size	Circle fit residuals analysis for sample listed in Tag column						
				Range full	Range inliers	SD full	SD inliers	MAD full	MAD inliers	Center (x,y)
		in	in	in	in	in	in	in	in	thou
c01	z-axis	0.0004	473	0.0045	0.0033	0.0007	0.0007	0.0005	0.0005	-0.2, 0.3
c02	z-axis	0.0009	585	0.0050	0.0050	0.0010	0.0010	0.0007	0.0007	-0.7, 0.5
c03	z-axis	0.0005	612	0.0078	0.0073	0.0014	0.0013	0.0009	0.0009	-0.5, 0.1
c04	z-axis	0.0001	921	0.0056	0.0031	0.0007	0.0006	0.0004	0.0004	-0.1, 0.1
c05	z-axis	0.0002	711	0.0045	0.0037	0.0007	0.0006	0.0004	0.0004	0.1, -0.2
c06	z-axis	0.0017	531	0.0076	0.0063	0.0014	0.0014	0.0010	0.0010	-0.5, 1.6
c07	z-axis	0.0004	676	0.0100	0.0075	0.0013	0.0012	0.0008	0.0008	0.4, 0.2
c08	z-axis	0.0009	1119	0.0126	0.0077	0.0014	0.0013	0.0008	0.0008	0.4, -0.8
c09	z-axis	0.0008	1305	0.0094	0.0068	0.0012	0.0011	0.0008	0.0008	0.8, -0.0
c10	z-axis	0.0011	878	0.0090	0.0073	0.0013	0.0012	0.0009	0.0009	1.1, -0.2
c01	c06	0.0013	473	0.0045	0.0033	0.0007	0.0007	0.0005	0.0005	0.2, -1.3
c02	c07	0.0012	585	0.0050	0.0050	0.0010	0.0010	0.0007	0.0007	-1.1, 0.3
c03	c08	0.0013	612	0.0078	0.0073	0.0014	0.0013	0.0009	0.0009	-0.9, 0.9
c04	c09	0.0008	921	0.0056	0.0031	0.0007	0.0006	0.0004	0.0004	-0.8, 0.2
c05	c10	0.0010	711	0.0045	0.0037	0.0007	0.0006	0.0004	0.0004	-1.0, 0.0

Concentricity measurements in z-plane

Tag	Reference	Deviation	Sample size	Circle fit residuals analysis for sample listed in Tag column						
				Range full	Range inliers	SD full	SD inliers	MAD full	MAD inliers	Center (x,y)
		in	in	in	in	in	in	in	in	thou
c01	z-axis	0.0005	503	0.0048	0.0047	0.0009	0.0009	0.0005	0.0005	-0.3, 0.4
c02	z-axis	0.0011	735	0.0076	0.0064	0.0012	0.0012	0.0010	0.0010	-0.9, 0.6
c03	z-axis	0.0006	691	0.0094	0.0081	0.0015	0.0015	0.0010	0.0010	-0.6, 0.1
c04	z-axis	0.0002	922	0.0055	0.0034	0.0007	0.0006	0.0004	0.0004	-0.1, 0.1
c05	z-axis	0.0002	882	0.0059	0.0051	0.0010	0.0009	0.0006	0.0006	0.2, -0.2
c06	z-axis	0.0017	535	0.0105	0.0097	0.0025	0.0025	0.0021	0.0020	-0.5, 1.6
c07	z-axis	0.0006	837	0.0100	0.0082	0.0016	0.0014	0.0011	0.0011	0.5, 0.3
c08	z-axis	0.0009	1232	0.0142	0.0086	0.0018	0.0016	0.0012	0.0011	0.4, -0.8
c09	z-axis	0.0008	1309	0.0094	0.0067	0.0012	0.0011	0.0008	0.0007	0.8, -0.0
c10	z-axis	0.0015	1129	0.0103	0.0081	0.0016	0.0015	0.0011	0.0010	1.5, -0.2
c01	c06	0.0012	503	0.0048	0.0047	0.0009	0.0009	0.0005	0.0005	0.1, -1.2
c02	c07	0.0015	735	0.0076	0.0064	0.0012	0.0012	0.0010	0.0010	-1.5, 0.3
c03	c08	0.0014	691	0.0094	0.0081	0.0015	0.0015	0.0010	0.0010	-1.0, 0.9
c04	c09	0.0009	922	0.0055	0.0034	0.0007	0.0006	0.0004	0.0004	-0.8, 0.2
c05	c10	0.0013	882	0.0059	0.0051	0.0010	0.0009	0.0006	0.0006	-1.3, 0.0